[3] Where the '*ruber*' meets the road: Using the [4] genome of the Red Diamond Rattlesnake to [5] unravel the evolutionary processes driving venom [6] evolution

Samuel R. Hirst[1] | **Rhett M. Rautsaw[1,2]** | **Cameron M. VanHorn[1]** | **Marc A. Beer[2]** | **Preston J. McDonald[1]** | **Ramsés Alejandro Rosales-García[3]** | **Bruno Rodriguez Lopez[4]** | **Alexandra Rubio [7] Rincón[4]** | **Hector Franz-Chávez[5]** | **Víctor Vásquez-Cruz[6,7]** | **Alfonso Kelly-Hernández[7]** | **Andrew Storfer[2]** | **Miguel Borja[4]** | **Gamaliel Castañeda-Gaytán[4]** | **Paul B. Frandsen[8]** | **Christopher L. Parkinson[3]** | **Jason L. Strickland[9]** | **Mark J. Margres[1]**

[1]Department of Integrative Biology, University of South Florida, Tampa, FL, USA

[2]School of Biological Sciences, Washington State University, Pullman, WA, USA

[3]Biological Sciences Department, Clemson University, Clemson, SC, USA

[4]Facultad de Ciencias Biológicas, Universidad Juárez del Estado de Durango, Durango, MX

[5]Herp.MX©, Colima, MX

[6]Facultad de Ciencias Biológicas y Agropecuarias, Universidad Veracruzana, Veracruz, MX

[7]PIMVS Herpetario Palancoatl, Veracruz, MX

[8]Department of Plant and Wildlife Sciences, Brigham Young University, Provo, UT, USA

[9]Department of Biology, University of South Alabama, Mobile, AL, USA

Correspondence
Samuel R. Hirst; Mark J. Margres
Email: hirsts@usf.edu;
margres@usf.edu

Funding information
See below

Understanding the proximate and ultimate causes of phenotypic variation is fundamental in evolutionary research, as such variation provides the substrate for selection to act upon. Although trait variation can arise due to selection, the importance of neutral processes is sometimes understudied. We presented the first reference-quality genome of the Red Diamond Rattlesnake (*Crotalus ruber*) and used range-wide 'omic data to estimate the degree to which neutral and adaptive evolutionary processes shaped venom evolution. We characterized population structure and found substantial genetic differentiation across two populations, each with distinct demographic histories. We identified significant differentiation in venom expression across age classes with substantially reduced but discernible differentiation across populations. We then used conditional redundancy analysis to test whether venom expression variation was best predicted by neutral divergence patterns or geographically-variable (a)biotic factors. Snake size was the most significant predictor of venom variation, with environment, prey availability, and neutral sequence variation also identified as significant factors, though to a lesser degree. By directly including neutrality in the model, our results confidently highlight the predominant, yet not singular, role of life history in shaping venom evolution.

Keywords: Transcriptomics, Population genomics, Ontogeny, Venom

1 | SIGNIFICANCE

Although the neutral theory of molecular evolution has provided a null model for >50 years when examining the genetics underlying phenotypes, neutral processes are not always explicitly incorporated into trait-based analyses. Snake venoms evolve quite rapidly and are often assumed to be evolving solely under strong directional selection. Here, we present the first reference-quality genome of the Red Diamond Rattlesnake and use range-wide 'omic data to estimate the degree to which neutral and adaptive evolutionary processes shape venom evolution. We found that life history evolution was the dominant force underlying venom variation. Following life history, however, neutral sequence variation explained comparable variation to both biotic and abiotic factors, suggesting that neutral processes play a more prominent role than previously thought.

2 | INTRODUCTION

Natural populations often exhibit exceptional degrees of phenotypic variation (Darwin, 1859; Nevo, 1978), such as body color of strawberry poison frogs (Summers *et al.*, 2003; Yang *et al.*, 2019), body and beak size of Galapagos Island finches (Darwin, 1859; Grant and Grant, 2002), and levels of salinity resistance in salt marsh plants (Hester *et al.*, 2001) among others (Hoekstra *et al.*, 2006; Dickson *et al.*, 2017). Such variation can be the product of adaptive and/or neutral evolutionary processes (Lande, 1976). Neutrality often serves as the evolutionary null hypothesis (Fisher, 1930; Ohta, 1973; Nei, 2005; Müller *et al.*, 2022; Kimura, 1968), as it provides a baseline against which the effects of natural selection can be measured (Zhang, 2018; Rohlfs *et al.*, 2014; Serra *et al.*, 2013). Phenotypic variation, however, is frequently explored solely within the framework of selection and adaptation (Gould and Lewontin, 1979; Smith *et al.*, 2023; Brodie *et al.*, 2002; Williams *et al.*, 2003; Hanifin *et al.*, 2008), even when such variation may be the product of neutral evolutionary processes via geographically-limited dispersal and consequent gene flow (Lande, 1976; Alexander *et al.*, 2006). Indeed, a textbook example of phenotypic variation assumed to be adaptive is toxin production in rough-skinned newts (*Taricha granulosa*). Newt toxin production may be a response to coevolutionary interactions with a toxin-resistant predator, the common garter snake (*Thamnophis sirtalis*; Brodie and Brodie, 1990; Brodie *et al.*, 2002, 2005; Williams *et al.*, 2010, 2003). Recently, a robust statistical framework accounting for demographic histories and population structure demonstrated that *T. granulosa* toxicity levels were more significantly predicted by population structure and isolation-by-distance (IBD) rather than resistance levels of *T. sirtalis* (Hague *et al.*, 2020), indicating that neutral evolutionary processes were substantially contributing to variation in toxin production. The relationship between population structure and toxin production in *T. granulosa* highlights the importance of determining whether other traits assumed to be evolving under strong selection actually exhibit patterns consistent with *only* adaptive evolution (Zhang, 2018).

Recently, snake venom has emerged as an effective system for studying adaptive evolution (Mason *et al.*, 2022; Margres *et al.*, 2017a; Rao *et al.*, 2022; Arbuckle, 2020). However, neutral evolution in this system is occasionally untested (Smith *et al.*, 2023; Davies and Arbuckle, 2019; Cipriani *et al.*, 2017; Barlow *et al.*, 2009; Smiley-Walters *et al.*, 2017; Sanz *et al.*, 2006) despite evidence that neutral processes, such as genetic drift, may play a role in shaping venom characteristics (Casewell *et al.*, 2020; Aird *et al.*, 2017; Sasa, 1999; Rao *et al.*, 2022). Snake venom is a complex, polygenic trait composed of 40−100 proteinaceous toxins used for prey immobilization, digestion, and defense (Casewell *et al.*, 2011; Mackessy, 2021; Barlow *et al.*, 2009; Daltry *et al.*, 1996). Despite the complex genomic architecture of venom (Margres *et al.*, 2021a; Schield *et al.*, 2019; Hogan *et al.*, 2024), toxin gene expression is specific to venom glands (Rokyta *et al.*, 2015), with differences in expression having clear, functional effects on the venom phenotype (Margres *et al.*, 2017a; Holding *et al.*, 2016; Barlow *et al.*, 2009; Casewell *et al.*, 2020; Smiley-Walters *et al.*, 2017). Venom expression exhibits extensive variation across different species (Casewell *et al.*, 2014; Durban *et al.*, 2017; Pla *et al.*, 2019; Senji Laxme *et al.*, 2019; Jackson and Fry, 2016; Jackson *et al.*, 2016; Margres *et al.*, 2015a; Holding *et al.*, 2021), populations of the same species (Massey *et al.*, 2012; Smith *et al.*, 2023; Margres *et al.*, 2019, 2015a; Holding *et al.*, 2018), and life histories (Durban *et al.*, 2017; Margres *et al.*, 2015a,b; Wray *et al.*, 2015; Rokyta *et al.*, 2017; Schonour *et al.*, 2020; Barlow *et al.*, 2009; Borja *et al.*, 2018; Andrade and Abe, 1999; Cipriani *et al.*, 2017; Modahl *et al.*, 2016; Alape-Girón *et al.*, 2008); venom expression variation at all three scales has also been shown to be the result of genetic rather than environmental (i.e., plastic) effects (Margres *et al.*, 2015b; Gibbs *et al.*, 2009). Abiotic and/or biotic selective pressures, such as differences in environment (Margres *et al.*, 2021b; Strickland *et al.*, 2018; Siqueira-Silva *et al.*, 2021), diet (Holding *et al.*, 2018, 2021; Mackessy *et al.*, 2003; Schonour *et al.*, 2020), or prey venom resistance (Margres *et al.*, 2017a; Holding *et al.*, 2016; Barlow *et al.*, 2009), may produce such variation. Antagonistic coevolutionary interactions with prey have been associated with venom expression variation in certain cases (Margres *et al.*, 2017a; Holding *et al.*, 2016; Barlow *et al.*, 2009); however, prey-driven selection is often assumed to produce venom expression variation without sufficient empirical evidence (e.g., Smith *et al.*, 2023). Determining whether venom expression variation is adaptive requires both precise knowledge of diet and quantitative and functional measurements of venom effectiveness in multiple prey species and populations, making it exceptionally difficult to test (Margres *et al.*, 2017a; Holding *et al.*, 2016; Barlow *et al.*, 2009; Casewell *et al.*, 2020; Smiley-Walters *et al.*, 2017). Consequently, venom studies often rely on methods for detecting signatures of selection such as dN/dS ratios (Juárez *et al.*, 2008; Margres *et al.*, 2013; Rokyta *et al.*, 2013; Mason *et al.*, 2020; Zhao *et al.*, 2021), but changes to gene-expression patterns have, in general, been found to explain a disproportionate amount of venom expression variation (Margres *et al.*, 2016a, 2017a,b), consistent with other traits (Gompel *et al.*, 2005; Fraser, 2013; Konczal *et al.*, 2015). Nevertheless, venom expression variation should not be exclusively attributed to adaptive evolution without investigating the potential role of neutral evolutionary processes (Sasa, 1999; Rao *et al.*, 2022; Casewell *et al.*, 2020). Much like the variable toxin production observed across *T. granulosa* populations, geographic variation in snake venom expression may be erroneously attributed solely to selection, whereas it may arise, at least in part, from neutral evolutionary processes.

The Red Diamond Rattlesnake (*Crotalus ruber*) exhibits ontogenetic and geographic venom variation (Straight *et al.*, 1992), making it an excellent focal species for investigating the contributions of neutral and adaptive processes on snake venom evolution. *Crotalus ruber*

TABLE 1 Genome assembly statistics for *C. ruber*. All metrics are for the *de novo* assembly except "Number of scaffolds", "Scaffold N50", and "bp anchored to chromosomes" which represent metrics for the RagTag assembly to *C. adamanteus*. BUSCO metrics are shown as complete (C), duplicated (D), fragmented (F), and missing (M). Genome assembly available at NCBI PRJNA1051499.

| Metric	
Assembly size (Gb)	1.59
Number of contigs	1, 126
Contig N50 (Mb)	6.25
Contig L50	65
Number of scaffolds	111
Scaffold N50 (Mb)	206.58
bp anchored to chromosomes (Gb)	1.57 (98.7%)
Phred quality score (Q)	55
k-mer completeness %	96
BUSCO Vertebrata (C|D|F|M) %	96.5 | 1.0 | 1.1 | 2.4
BUSCO Sauropsida (C|D|F|M) %	93.0 | 1.2 | 1.2 | 5.8
CG content, %	39.8
Repeat content, %	49.07
Protein-coding genes	20,771
Putative venom protein-coding genes	94

is a large-bodied pitviper found in western North America ranging from San Bernadino County, California, USA, south throughout the Baja California peninsula and various islands. Habitat throughout its range varies extensively (Grismer, 2002), and its prey composition, which includes primarily small to medium-sized mammals, is well-characterized (Dugan and Hayes, 2012). Two mainland subspecies are recognized: *C. r. ruber* extends from the northern range edge to the central region of the Baja peninsula, and *C. r. lucasensis* inhabits the southern third of the Baja peninsula (Figure 1). The current subspecies definitions are based on morphological (Grismer, 2002) and genetic differentiation, with divergence occurring ∼570 ka before present (Harrington *et al.*, 2018). Although *C. ruber* exhibits venom variation in specific protein families across its geographic range and life history (Pozas-Ocampo *et al.*, 2020; Straight *et al.*, 1992), variation across the complete venom phenotype as well as the evolutionary processes producing such variation have yet to be investigated.

In this study, we investigated the evolutionary processes, both adaptive and non-adaptive, that may have produced variation in a trait that is often assumed to be evolving under strong directional selection. We aimed to 1) generate the first reference *C. ruber* genome for use in downstream analyses, 2) characterize neutral population structure and demographic history, 3) quantify venom expression variation across populations and life history stages, and 4) determine the relative contributions of neutral evolutionary processes, geographically-variable abiotic and/or biotic factors, and life history in explaining venom expression evolution through robust statistical models. If venom is rapidly evolving due to selection, we expect decoupling of patterns produced by neutral evolutionary processes, such as population structure and IBD (Wright, 1943; Keller *et al.*, 2009; Williams *et al.*, 1988), with venom variation spatially, as demonstrated previously (Margres *et al.*, 2019). Specifically, we would expect patterns of venom variation to correlate with patterns of variation in abiotic and/or biotic factors such as dietary composition or climate (Holding *et al.*, 2018). Conversely, if venom is evolving due to neutral processes, we expect a strong correlation between neutral sequence variation and venom variation, similar to what was found for toxin-production levels in newts (Hague *et al.*, 2020). Overall, our approach integrating diverse data types from multiple individuals across the range will allow us to identify the most significant factors driving venom evolution within a species.

3 | RESULTS

3.1 | De Novo Genome Assembly and Annotation

We generated a reference *C. ruber* genome using PacBio HiFi reads (∼20× coverage) for a subadult male collected within the *C. r. ruber* range near Bahía de los Ángeles, Baja California, MX (Figure 1). Genome assembly length was 1.59 Gb (1,126 contigs, N50 of 6.25 Mb, L50 of 65; Table 1). We calculated additional genome quality assessment metrics, such as phred quality score (55), k-mer completeness (96%), and BUSCO (96.5% complete Vertebrata; 93.0% complete Sauropsida; Table 1). To achieve a chromosome-level assembly, we scaffolded the *C. ruber* assembly to the chromosome-level assembly of the Eastern Diamondback Rattlesnake (*C. adamanteus*; Hogan *et al.*, 2024) using RagTag (Alonge *et al.*, 2022). The number of contigs in the assembly was reduced ∼10× to 111 scaffolds (N50 of 206.58 Mb), and all 17 autosomes assembled for *C. adamanteus* were assembled for *C. ruber*. Because our genome individual was male, only the Z sex chromosome was assembled (Figure 2A). We annotated the genome and identified 20,771 protein-coding

Crotalus ruber ruber

Crotalus ruber lucasensis
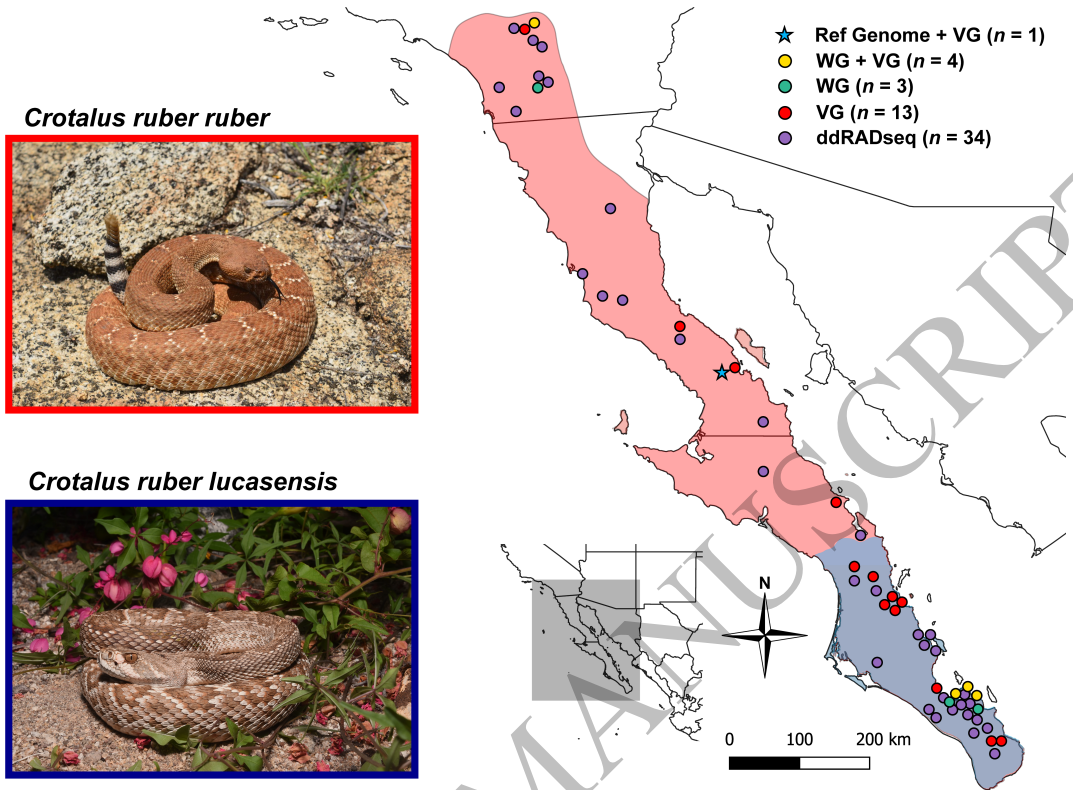
FIGURE 1 Distribution and sampling map of *Crotalus r. ruber* (red map shading) and *C. r. lucasensis* (blue map shading). Color of sampling point is based on the types of data generated for the individual sampled at that location. Abbreviations: Ref Genome, PacBio HiFi genome sequencing; WG, short-read whole-genome sequencing; VG, venom-gland transcriptomes; ddRADseq, double digest restriction-site associated DNA Sequencing. Snake image credits: Ricardo Ramírez Chaparro.

genes including 94 putative toxin genes within 14 toxin families (Figure 2A). Multiple toxin families were found on microchromosomes (chromosomes 9−18 in Figure 2A) as large tandem arrays, consistent with toxin genomic organization in other rattlesnakes (Margres *et al.*, 2021a; Hogan *et al.*, 2024; Schield *et al.*, 2019).

3.2 | Population Genomics Identifies Distinct Populations and Evolutionary Histories

We used conStruct (Bradburd *et al.*, 2018) across 39 individuals (2,241 SNPs) to characterize population structure (Figure 2B-C). Spatial models invariably had higher predictive accuracy than nonspatial models, with predictive accuracy reaching an asymptote at $K = 2-3$ genetic clusters (Supporting Information Figure S1). For the spatial models, additional genetic clusters beyond $K = 2$ explained <5% of total genetic covariance, suggesting that $K = 2$ was an appropriate choice for characterizing population genetic structure (Figure 2B). After cross-validation, we fit final spatial models using the full dataset for $K = 2$ and $K = 3$. For $K = 2$, populations were spatially sorted by latitude (Figure 2B), with contact at $\sim 26°$N latitude, relatively consistent with current *C. ruber* subspecies delineation (Figure 1; Grismer, 2002). A similar pattern was observed for $K = 3$ (Figure 2C), with additional weak population structure at the northern range edge. We calculated the fixation index (F_{ST}) between the populations for $K = 2$ in conStruct (hereinafter referred to as the north and south populations) using the full genomic dataset (north $n = 19$; south $n = 22$; 5,284 SNPs) as well as the reduced genomic dataset (north $n = 18$; south $n = 21$; 2,241 SNPs) used specifically for conStruct. We found that $F_{ST} = 0.295$ and 0.301, respectively. We also visualized patterns of sequence dissimilarity using the full genomic dataset ($n = 41$; 5,284 SNPs) using PCoA. Individuals clustered according to the population structure identified in conStruct; southern individuals clustered tightly along both PCo1 and PCo2 while northern individuals clustered tightly along PCo1, but with increased variance along PCo2 (Supporting Information Figure S2A).

Next, we estimated effective migration surfaces (EEMS; Petkova *et al.*, 2016) using the full genomic dataset (*n* = 41; 5,284 SNPs) to explore spatially variable migration rates across the landscape and visualize departures from IBD (Figure 2D). We observed three areas of relative reductions in gene flow: (1) the Peninsular Ranges of Southern California, (2) the Vizcaíno Desert of the Baja Peninsula, and (3) the current *C. ruber* subspecies boundary at $\sim$ 26°N latitude near the town of Loreto, BCS, MX (Figure 2D).

Lastly, we estimated demographic histories for the north (*n* = 3) and south (*n* = 5) populations using the Parwise Sequentially Markovian Coalescent model (PSMC; Figure 2E; Li and Durbin, 2011) on our whole-genome data. Effective population size (N_e) decreased in both populations between $\sim 100-200$ ka before present and continued to decrease during the last glacial period (Broecker and Hemming, 2001) between $\sim 50-100$ ka for the northern population while stabilizing in the southern population (Figure 2E).

3.3 | Venom Expression Varies Extensively Across Life History and Less So Across Geographic Space

We conducted a PCA on the venom proteomic data for 20 individuals (Supporting Information Table S1) and found that PC1 (65%) was primarily associated with SVL, with individuals clustering into two groups separated at $\sim$65 cm SVL (Supporting Information Figure S3). Indeed, a linear regression showed that venom PC1 was significantly correlated with SVL (p < 0.001, adj-R^2 = 0.82; Supporting Information Figure S3B). To test for venom protein expression differentiation across age class ($\leq$ 65 cm juvenile) and population (northern and southern populations as defined in conStruct), we conducted a PERMANOVA. Only ontogeny was significant (p < 0.001, R^2 = 0.65; adult *n* = 14; juvenile *n* = 6); neither population (p = 0.194, R^2 = 0.03; north *n* = 11; south *n* = 9) nor the interaction between age and population (p = 0.275, R^2 = 0.02) were significant. Overall, our proteomic analyses revealed that, at the trait level, venom expression was significantly different between age classes but not significantly different between populations.

To identify the specific toxin genes underlying ontogenetic venom variation and determine whether any individual toxin genes were significantly differentially expressed (DE) between populations, we generated venom-gland transcriptome data for 18 individuals across the range (Figure 3). We first verified that the venom gland transcriptomic data exhibited similar patterns to those observed in the venom proteomic data by reconducting both PCA and PERMANOVA (Figure 3A;B). PC1 (31%) was again significantly and positively correlated with SVL (p <0.001, adj-R^2 = 0.65; Figure 3A), and only ontogeny was significant in the PERMANOVA (p = 0.005, R^2 = 0.31; adult *n* = 13; juvenile *n* = 5); neither population (p = 0.200, R^2 = 0.07; north *n* = 12; south *n* = 6) nor the interaction between age and population (p = 0.590, R^2 = 0.02) were significant.

We identified specific genes that were significantly DE across populations (Figure 3C) and age classes (Figure 3D). Between populations (north *n* = 12; south *n* = 6), four toxin genes were significantly DE, with all four genes (*C-type lectin [CTL]–1, CTL–2, snake venom metalloproteinase [SVMP]–mad–6, SVMP–mpo–1*) exhibiting higher expression in the northern population. Between age classes (adult *n* = 13; juvenile *n* = 5), while accounting for population, 27 toxin genes were significantly DE. The majority (*n* = 21) of the genes were biased toward adults (i.e., more highly expressed in adults than juveniles), with most genes belonging to the *SVMP* (*n* = 9) and *CTL* (*n* = 6) toxin families. Most juvenile-biased toxin genes (*n* = 6) belonged to the myotoxin gene family (*n* = 3). See Supporting Information Table S2 for details of all DE transcripts between age groups and populations.

3.4 | Conditional Redundancy Analysis Identifies Life History as the Most Predominant Driver of Venom Evolution

To determine the relative roles of putatively neutral and adaptive evolutionary processes in driving venom expression evolution, we used conditional RDA to estimate the effects of nontoxin sequence variation (our proxy for neutrality; Supporting Information Figure S2A-C, S4), toxin sequence variation, abiotic environmental factors, and prey data (availability and phylogenetic distance) on multivariate venom expression data.

First, we used PCoA to determine whether (1) nontoxin SNPs accurately reflected patterns of neutral genomic sequence variation and (2) patterns of nontoxin sequence variation were robust to the inclusion of nonsynonymous variants. Patterns of sequence variation under PCoA were consistent among neutral genomic SNPs, nontoxin synoynmous SNPs, and nontoxin SNPs including all variant types (Supporting Information Figure S2). Additionally, correlation between PCo1 of nontoxin synonymous SNPs and PCo1 of all nontoxin SNPs was highly significant (Supporting Information Figure S4; p < 0.001; R^2 = 0.97). Therefore, nontoxin SNPs including all variant types served as a valid proxy for neutral patterns of genetic divergence.

Using conditional RDA with toxin gene read count estimations from HTSEQ-count as the multivariate response variable, the full model, including all variables, was significant (p = 0.002; adj-R^2 = 0.73; Table 2), indicating that our model captured at least one or more variables that significantly explained venom expression variation. The marginal (i.e., best) model (adj-R^2 = 0.54) as determined from forward model selection revealed that SVL (p = 0.003; adj-R^2 = 0.30), prey availability (NMDS2; p = 0.010; adj-R^2 = 0.14), and abiotic factors (Bioclim PC1; p = 0.012; adj-R^2 = 0.10) were the most significant predictors of venom expression variation (Table 2).

Similarly, using read count estimations from Stringtie2 as the multivariate response variable, the full model, including all variables, was again significant (p = 0.003; adj-R^2 = 0.66; Table 3). The marginal model (adj-R^2 = 0.62) as determined from forward model selection differed slightly from the best model using HTSeq-count data as input; here, SVL (p = 0.001; adj-R^2 = 0.44), abiotic factors (Bioclim PC1; p = 0.001; adj-R^2 = 0.12), and nontoxin sequence variation (Nontoxin PCo1; p = 0.020; adj-R^2 = 0.06) were the most significant predictors of venom expression variation (Table 3).
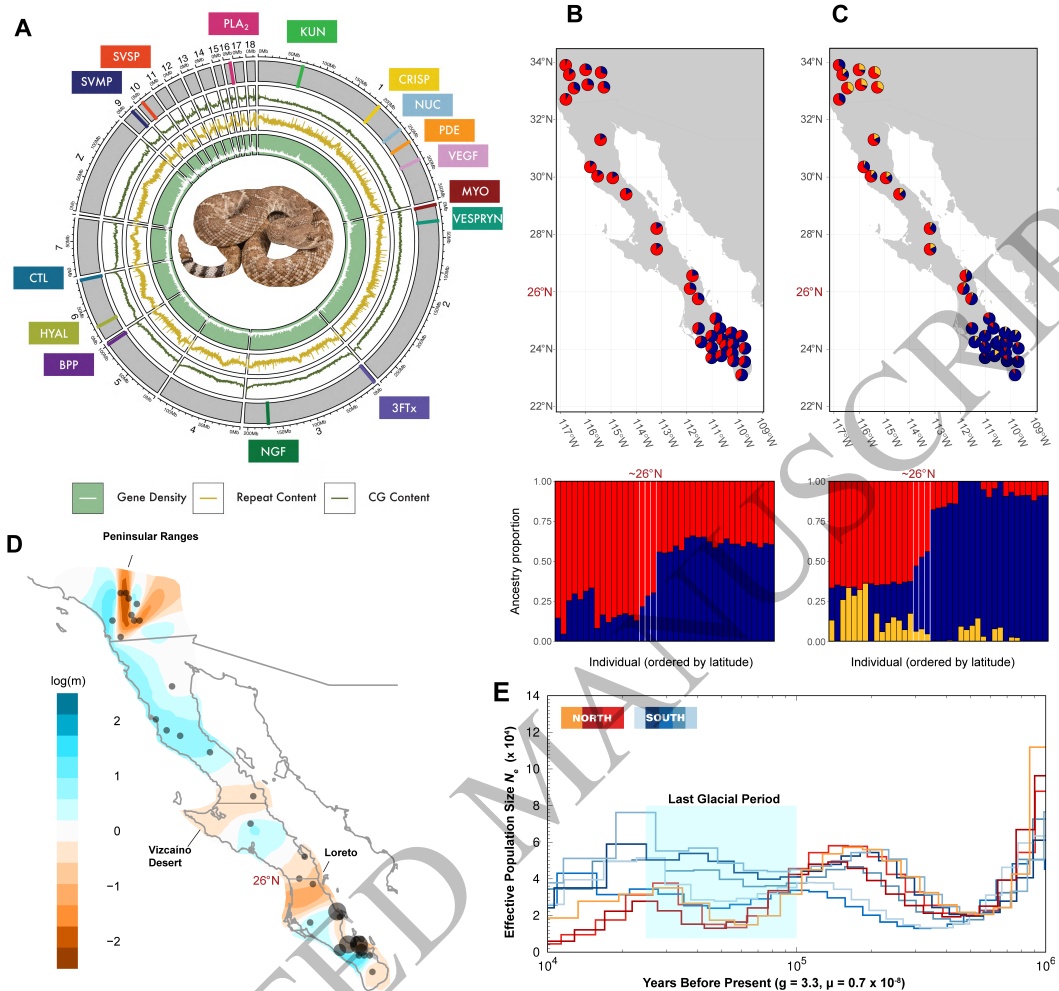
FIGURE 2 Reference-genome assembly and genomic sequencing of *C. ruber* reveals two genetically distinct populations with unique demographic histories. (A) Circos plot of the RagTag reference genome assembly displaying gene density, repeat content, CG content, and toxin gene families mapped to chromosome scaffolds as represented by corresponding colored lines. Toxin families are (ordered by chromosome): KUN, Kunitz-type toxin; CRISP, cytesine-rich secretory protein; NUC, nucleotidase; PDE, phosphodiesterase; VEGF, vascular endothelial growth factor; MYO, myotoxin; 3FTx, three-finger toxin; NGF, nerve growth factor; BPP, bradykinin-potentiating peptide; HYAL, hyaluronidase; CTL, C-type lectin; SVMP, snake venom metalloproteinase; SVSP, snake venom serine proteinase; PLA$_2$, phospholipase A$_2$. (B–C) Population structure characterized from short-read whole genome sequencing (WGS) and ddRADseq data using ConStruct spatial models with (B) K = 2 and (C) K = 3. Maps depict individuals as pie charts reflecting ancestry proportions contributed by each genetic cluster. (D) Estimated effective migration surface from WGS and ddRADseq data using EEMS. Shading indicates areas with relatively high (orange) and low (blue) landscape resistance to gene flow compared to a null area-wide model of isolation-by-distance (IBD). Plotted values of log(*m*) are effective migration rates relative to the overall migration rate across the study area. Circles represent sampling locations, and circle size corresponds to sampling density. (E) Estimates of demographic histories across the two distinct populations from panel B. Lines represent effective population size (N_e) estimated from eight individuals using a generation length of 3.3 years and a mutation rate of 0.007 per lineage per million years. Colors indicate N_e estimates of individuals sampled from the northern population (warm) and southern population (cool; as determined in panel B). Contact zone ($\sim 26^\circ$N) is indicated throughout.

TABLE 2 Results of the conditional RDA for venom gland transcriptome normalized read count data from HTSeq-count as the response variable. Marginal model was identified using forward model selection on all explanatory variables. Results for all variables can be found in Supporting Information Table S3.

	F	p-value	adj-R^2
Full Model	5.521	0.002	0.73
Marginal Model			0.54
SVL	8.32	0.003	0.30
Prey NMDS2	5.17	0.01	0.14
Bioclim PC1	4.49	0.012	0.10

TABLE 3 Results of the conditional RDA for venom gland transcriptome normalized read count data from stringtie2 as the response variable. Marginal model was identified using forward model selection on all explanatory variables. Results for all variables can be found in Supporting Information Table S3.

	F	p-value	adj-R^2
Full Model	4.29	0.003	0.66
Marginal Model			0.62
SVL	14.24	0.001	0.44
Bioclim PC1	5.38	0.001	0.12
Nontoxin PCo1	3.42	0.02	0.06

3.5 | Life History Best Explains Expression Evolution Across Individual Toxin Gene Families

We determined whether expression variation of the six most abundantly expressed toxin families (bradykinin-potentiating peptide [BPP], C-type lectin [CTL], Myotoxin, phospholipase A$_2$ [PLA$_2$], snake venom metalloproteinase [SVMP], snake venom serine proteinase [SVSP]) were significantly correlated with different explanatory variables. Variation across all toxin families, as identified in the marginal models, was significantly correlated with SVL (Table 4). Nontoxin sequence variation was also found to be a significant predictor of CTL, Myotoxin, and SVMP expression. Abiotic variation (Bioclim PC1) was the most significant predictor of PLA$_2$ expression variation. Prey was identified as a significant predictor of expression variation in BPP and SVSP toxin families, with prey availability (NMDS2) predicting BPP expression variation, and prey mean phylogenetic distance (MPD) predicting SVSP expression variation. See Supporting Information Table S3 for detailed results of conditional RDAs for individual toxin families.

4 | DISCUSSION

4.1 | Assembly and Annotation of Reference Quality *C. ruber* Genome

Genomic content of the reference genome assembly was similar to that of other snake assemblies (Vonk *et al.*, 2013; Yin *et al.*, 2016; Schield *et al.*, 2019; Suryamohan *et al.*, 2020; Margres *et al.*, 2021a; Li *et al.*, 2021; Hogan *et al.*, 2024; Westeen *et al.*, 2023). Notably, the *C. ruber* genome assembly displayed improved contiguity compared to several prior *Crotalus* assemblies, exhibiting a higher contig N50 and fewer total contigs compared to *C. tigris* (Margres *et al.*, 2021a) and *C. viridis* (Schield *et al.*, 2019). Overall, the accurate and contiguous reference-quality genome for *C. ruber* enabled us to robustly explore the effects of multiple evolutionary processes on venom evolution using reference-based genomic and transcriptomic analyses.

4.2 | Population Genomics Reveals Two Genetically Distinct Populations with Unique Evolutionary Histories

We identified two genetically distinct populations separated by latitude with contact at $\sim 26^\circ$N latitude near Loreto, BCS, MX (Figure 2B), consistent with previous results (Harrington *et al.*, 2018). Genetic differentiation between the two identified populations was extensive (F_{ST} = 0.295 - 0.301), with levels of fixation similar to that of highly genetically distinct populations of other North American vipers (Gibbs *et al.*, 1997; Schmidt, 2019; Margres *et al.*, 2019). Reduced gene flow compared to expectations under a model of IBD was observed at the northeastern range edge near the Peninsular Ranges (Figure 2D), which separate the California chaparral from the the Sonoran Desert. The Sonoran Desert serves as a barrier to migration for many terrestrial organisms (Brown *et al.*, 2009; Ernest *et al.*, 2003), and for *C. ruber* (Greenberg, 2002), the barrier likely exists due to climatic differences and competition with congenerics such as its sister taxon, the Western Diamondback Rattlesnake (*C. atrox*; Alencar *et al.*, 2016). Reduced gene flow was also observed near the Vizcaíno desert (Figure 2D). Numerous species of the Baja region exhibit population differentiation occurring at the Vizcaíno
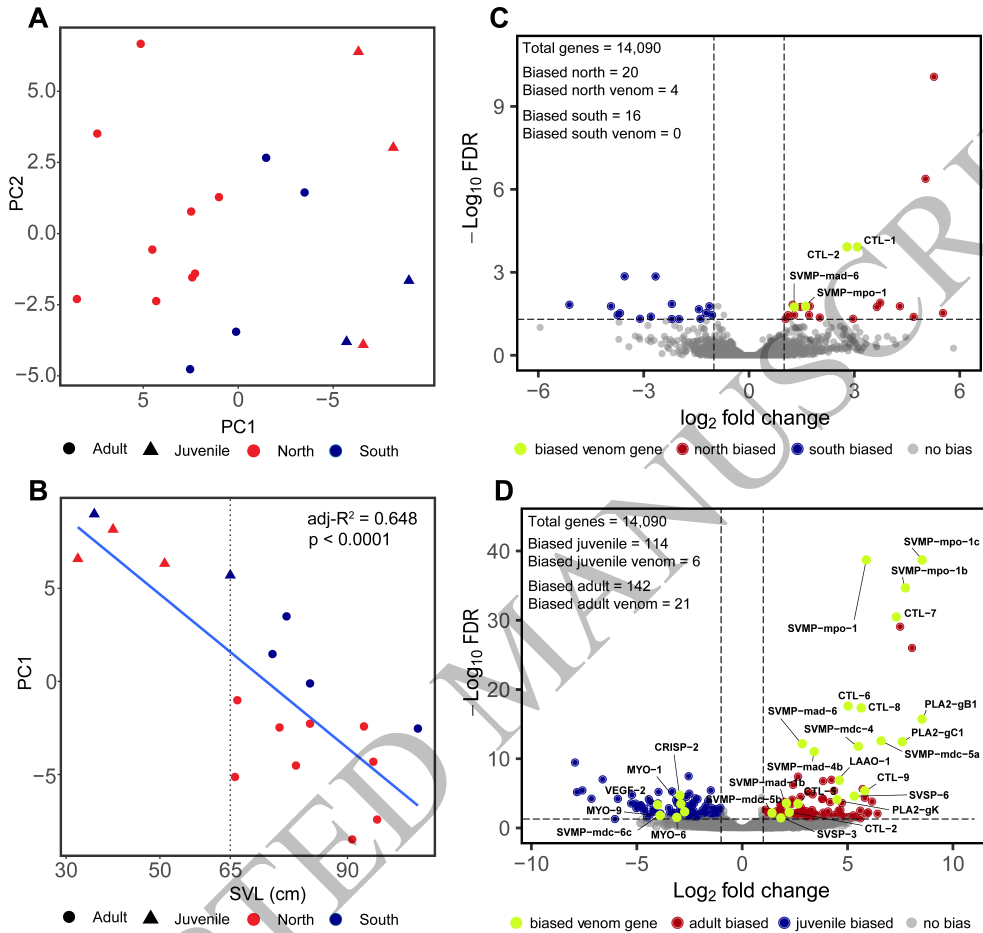
FIGURE 3 Differential venom expression across life history and geographic space in *C. ruber*. (A) Principal Component Analysis of venom gland transcriptome DESEQ2 normalized count data, and (B) Regression of Principal Component 1 (PC1) with snout-vent length (SVL). Dotted line at 65 cm SVL shows the cut-off used for age class designation. Proportion of variance accounted for in PC1 and PC2 was 31% and 13%, respectively. (C-D) Volcano plots of differential expression calculated from DESeq2 between populations (C) and age classes (D). Vertical dotted lines represent log2 fold change (LFC) $\geq$ 1, and horizontal dotted line represents $\alpha \leq 0.05$. Green points in each plot denote significantly differentially expressed toxin transcripts, and their placement denotes group bias. Abbreviations: SVL, snout-vent length; BPP, bradykinin-potentiating peptide; CRISP, cytesine-rich secretory protein; CTL, C-type lectin; MYO, myotoxin; PLA$_2$, phospholipase A$_2$; SVMP, snake venom metalloproteinase; SVSP, snake venom serine proteinase.

TABLE 4 Significant variables of the marginal models identified through forward model selection from conditional RDAs using the top six most abundantly expressed toxin families. Results for all variables in each family can be found in Supporting Information Table S3.

Toxin Family	Marginal Model	p-value	adj-R^2
BPP	SVL	0.010	0.31
	Prey NMDS2	0.008	0.22
CTL	SVL	0.004	0.32
	Nontoxin PCo1	0.015	0.15
Myotoxin	SVL	0.004	0.34
	Nontoxin PCo1	0.039	0.13
PLA$_2$	Bioclim PC1	0.001	0.38
	SVL	0.001	0.29
SVMP	SVL	0.007	0.27
	Nontoxin PCo1	0.013	0.18
SVSP	SVL	0.012	0.19
	Prey MPD	0.047	0.11

desert (Riddle *et al.*, 2000). Three hypotheses suggest that this region may serve as a major barrier to migration in multiple organisms due to (1) a proposed ancient transpeninsular seaway that bisected the peninsula during the late Miocene to middle Pleistocene, (2) isolation due to Pleistocene glacial–interglacial cycles, or (3) differences in rainfall patterns between the peninsular regions (reviewed in Dolby *et al.*, 2022). The Vizcaíno desert region, however, functions only as a minor barrier to migration in *C. ruber*, at least relative to the Peninsular Ranges and subspecies boundary at ∼ 26°N latitude (Figure 2D). The deviation of *C. ruber* population structure from the patterns exhibited by other species (Riddle *et al.*, 2000) was not associated with any apparent current or ancient topographic or geographic barriers to dispersal; rather, population structure has been proposed to be potentially linked with climatic fluctuations that occurred during the Pleistocene, resulting in temporary isolation of the two populations ∼450−510 ka before present until secondary contact ∼80 ka before present (Harrington *et al.*, 2018). N_e in the northern and southern populations appeared to concordantly increase during the potential period of climate-driven isolation (∼200−450 ka before present). At the time of purported secondary contact during the last glacial period (∼80 ka before present), N_e decreased in the northern population while remaining relatively stable in the southern population (Figure 2E). The observed differences in N_e between the two populations during the last glacial period suggests a pivotal role of climate-induced pressures on N_e and migration dynamics. Climate conditions were likely less favorable for snake survival in the northern range during glacial periods (Herbert *et al.*, 2001), potentially driving the previously isolated northern population south and leading to decreased N_e and renewed contact with the southern population. Due to the limitations of PSMC in resolving more recent demographic histories, however, inferences of N_e near the present may not be inferred accurately (Liu and Fu, 2015; Patton *et al.*, 2019; Nadachowska-Brzyska et al., 2016). Additional biogeographic analyses and sampling would be needed to further explore the distinct evolutionary histories of the two populations identified here.

4.3 | Venom Expression Differentiation Explained More by Ontogeny Than Genetic Population

Ontogenetic venom variation was much more pronounced than venom differentiation across populations. Indeed, age class explained ∼22× more variance in venom proteomic composition and ∼4× more variance in venom-gland transcriptome expression than population structure. The ontogenetic shift in venom expression occurred at ∼65 cm SVL (Supporting Information Figure S3) with continued variance throughout the life history of an individual, similar to other *Crotalus* species (Schonour *et al.*, 2020). Differential expression of individual genes revealed patterns of increased expression in SVMP and CTL toxin families in adults and the nothern population and increased expression of myotoxins in juveniles. Myotoxins are small, basic peptides that induce physiologic tetanus of skeletal muscles, particularly in mice, and likely play an important role in subduing prey (Brenes *et al.*, 1987; Mackessy *et al.*, 2003; Mackessy, 2021). SVMPs are a diverse family of large catabolic enzymes capable of causing severe damage to common structural proteins, inducing hemorrhage, and may aid in prey digestion (Slagboom *et al.*, 2017; Kini and Koh, 2016; Mackessy, 2021). Variable ontogenetic and geographic expression of SVMPs and myotoxins is observed in multiple *Crotalus* species (Margres *et al.*, 2015b; Straight *et al.*, 1991; Smith *et al.*, 2023), and such variation may be due to adaptive evolution. Adaptive differences may be produced by changes in prey preference at different life history stages (Mushinsky *et al.*, 1982) or optimal foraging strategy that promotes faster growth rates and reduces time spent in more vulnerable size classes (Klauber, 1997; Werner and Gilliam, 1984). For example, the production of large toxin enzymes such as SVMPs may be more metabolically costly (Mackessy, 1988), leading to limited expression in juveniles. Although the precise mechanism remains unknown, the venom phenotype was significantly variable across age classes with only a limited number of toxins exhibiting differential expression across populations, suggesting that changes in venom expression due to maturity may have greater ecological implications (i.e., differences in prey size and/or species) compared to changes across populations.

4.4 | Venom Variation Across Space Explained Primarily by Ontogeny with Significant but Reduced Effects of Other Selective Pressures and Neutral Processes

4.4.1 | Venom Variation Best Explained by Snake Size

Conditional redundancy analysis integrating snake size, environmental factors, prey availability, and prey phylogenetic distance revealed that snake size (i.e., ontogeny) best predicted multivariate venom expression variation, regardless of which read count estimation method was employed, consistent with our venom analyses described above. Similar to geographic venom variation, ontogenetic venom variation is commonly attributed to selection (Andrade and Abe, 1999; Cipriani *et al.*, 2017; Webber *et al.*, 2016; Gibbs *et al.*, 2011). Snakes, as gape limited predators, may select prey at different life history stages (Shine, 1991); therefore, the venom phenotype may adaptively shift as size increases to more effectively subdue and/or digest different, larger prey species (Margres *et al.*, 2015b). Variable efficacy of adult and juvenile venom in differing prey items is observed in multiple snake species (Mackessy, 1988; Margres *et al.*, 2016b; Andrade and Abe, 1999; Cipriani *et al.*, 2017; Borja *et al.*, 2018), suggesting that ontogenetic venom variation is often adaptive; however, the potential for neutral ontogenetic variation in snake venom has yet to be explored. Ontogeny may simply reflect developmental constraints which prevent the expression of otherwise beneficial traits or genes due to undeveloped key features or pathways (Barton and Boege, 2017; Gould and Lewontin, 1979; Fernandez-Lorenzo *et al.*, 1999). Indeed, similar to other rattlesnakes (Margres *et al.*, 2015b; Schonour *et al.*, 2020; Hogan *et al.*, 2024), we found that juvenile *C. ruber* venoms were simpler than adult venoms, with many more toxins upregulated in adults relative to juveniles (Figure 3E). Despite the current lack of understanding on developmental constraints in snake venom, a better comprehension of the regulatory architecture underlying ontogenetic venom variation (Hogan *et al.*, 2024) will enable future venom studies to incorporate such constraints into analyses of venom ontogeny.

Environmental differences also significantly explained venom expression variation using both read count estimation methods, consistent with previous work in other venomous snake species (Margres *et al.*, 2021b; Strickland *et al.*, 2018; Siqueira-Silva *et al.*, 2021). Overall, variation in annual temperature and temporal fluctuations in temperature were the most important environmental factors (Supporting Information Table S4; PC1). Snakes further north experience cooler overall temperatures and greater annual temperature fluctuations compared to snakes in the south which experience consistently warmer temperatures throughout the year. Climatic factors such as temperature have been found to influence snake feeding behavior and prey preferences (Vincent and Mori, 2008) which may in turn favor increased or decreased expression of certain toxin families that lead to more efficient feeding in particular climates. As described above, large toxin enzymes may aid in digestion; therefore, increased expression of these enzymes may be beneficial for snakes attempting to consume prey in cooler climates. Large enzymes such as SVMPs were more highly expressed in venoms from the northern population (Figure 3C), suggesting a potential correlation between expression of putatively digestion-aiding toxin enzymes and cooler temperatures. Alternatively, environmental abiotic factors may have more accurately captured changes in prey availability across geographic space (see below), suggesting that venom expression variation corresponded with environmentally-induced changes in prey availability. More detailed dietary analysis and toxicity measurements of different venoms in different prey under varying environmental conditions (e.g., assays conducted under different temperatures) would be needed to disentangle biotic and abiotic contributions to venom evolution.

Differences in prey availability were identified as significant within the marginal model using HTSeq-count derived data. Here, the significance of prey was primarily associated with an increase in prey availability at the northern range edge compared to individuals found throughout the Baja California Peninsula (Supporting Information Table S5; NMDS2). Venom composition and variation is frequently associated with differences in prey availability among populations (Smiley-Walters *et al.*, 2017; Holding *et al.*, 2016; Smith *et al.*, 2023; Margres *et al.*, 2017a; Gibbs and Mackessy, 2009; Barlow *et al.*, 2009; Daltry *et al.*, 1996; Robinson *et al.*, 2021), and variation in the number of available prey species between *C. ruber* populations appeared to contribute, in part, to venom evolution. Variables of prey availability and prey mean phylogenetic distance (MPD) within our model, however, assumed (1) that all *C. ruber* would consume a given prey item if present within its geographic location, and (2) all prey are equally abundant at each location. We acknowledge that these assumptions ignore ontogenetic changes in prey preference and/or geographic variation in prey abundance (Andrade and Abe, 1999; Cipriani *et al.*, 2017; Mackessy *et al.*, 2006; Dugan and Hayes, 2012). Additional diet information, including precise characterization of changes in prey composition across life history stages and variation in abundance for each prey species across space, would be necessary to confirm size/geographic-induced dietary constraints or preferences here.

Lastly, nontoxin sequence variation was identified as a significant predictor of multivariate venom expression variation with read count estimation from stringtie2. Although it was the weakest predictor of venom expression variation (adj-R^2 = 0.06) compared to ontogeny, abiotic factors, and biotic factors, its presence in the marginal model suggested that neutral evolutionary processes minimally explain some variation in the overall venom phenotype. Therefore, neutral evolutionary processes may have a diminished yet still significant impact on venom evolution. Significance of nontoxin sequence variation within the model, however, may be potentially confounded by strong population structure (Figure 2; Holding *et al.*, 2018); such population structure may have been the product of geographically-limited dispersal and genetic drift, and/or may be due to selective pressures causing reduced immigrant fitness (Garant *et al.*, 2007). Still, results of the marginal model suggested that neutral sequence variation, our proxy for neutral evolutionary processes, significantly explained some variation in the overall venom phenotype.

Although both read-count methods identified SVL as the most significant predictor of venom expression variation, the other significant predictors and their contributions to the model varied between the two methods. Specifically, nontoxin sequence variation was only a significant predictor for all toxins when using StringTie2 estimates; however, it was also a significant predictor across three specific toxin families (CTL, SVMP, and myotoxin) when using HTSeq-counts (Table 4). The significance of nontoxin sequence variation across both read-count methods provided confidence that the result was robust to any potential biases across methods. Why such differences occurred is not immediately clear, but varying sensitivities of the methods to different aspects of the data or inherent

differences in how these methods process read counts were suspected (See Materials and Methods). Further evaluation of each method, potentially including additional datasets and validation of findings through complementary approaches, would be necessary to better understand these discrepancies.

4.4.2 | Life History and Differing Secondary Factors Independently Contribute to Individual Toxin Family Evolution

Individual components of a complex trait like venom, such as specific toxin gene families, may evolve independently (Casewell *et al.*, 2011, 2020; Schield *et al.*, 2022); certain toxin families may play a more important role in specific aspects of feeding such as subduing, tracking, or digesting prey (Mackessy, 2021), leading to unique evolutionary trajectories from different evolutionary mechanisms. For example, prey resistance to certain toxins or toxin families (Robinson *et al.*, 2021; Holding *et al.*, 2016; Gibbs *et al.*, 2020; Margres *et al.*, 2017a) may lead to variable expression of those toxins whereas other toxins may evolve in response to abiotic conditions such as temperature (Margres *et al.*, 2021b; Strickland *et al.*, 2018; Tsai *et al.*, 2003).

We tested whether variation across individual toxin families was best explained by distinct factors compared to multivariate venom expression variation. SVL was identified in the marginal models of all toxin families individually, further demonstrating the significance of ontogenetically-induced venom variation in *C. ruber*. Variation in three of the toxin families (SVMP, CTL, myotoxin) was also significantly correlated with nontoxin sequence variation in addition to SVL (Table 4), suggesting that neutral evolutionary processes may contribute to variation across highly expressed toxin families of the venom phenotype. The relationship, however, may have been confounded by strong population structure (see above). Variation in the PLA_2 family was more significantly associated with environmental factors, particularly temperature, than SVL. Correlation between PLA_2 expression and environmental factors, especially those related to temperature, has been found in other Viperidae species (Margres *et al.*, 2021b; Strickland *et al.*, 2018; Tsai *et al.*, 2003) and may be associated with temperature-driven variation in snake feeding behavior, prey availability, and/or prey preference (Vincent and Mori, 2008). Consistent correlation observed across multiple species strongly implies a link between PLA_2 expression and environmental factors. Prey availability and prey phylogenetic distance was identified as a significant predictor of expression variation across the BPP and SVSP toxin families, suggesting that the evolution of these families may be strongly linked with prey-induced selective pressures.

The inclusion of snake size in the marginal models for all of the most abundantly expressed toxin families was concordant with patterns of venom expression variation, highlighting the importance of life history in shaping venom evolution in *C. ruber*. However, variation of secondary factors identified in the marginal models across multiple toxin families, such as BPPs, SVSPs, and PLA_2s, prompts further investigation into 1) why certain toxin families exhibit distinct putative selection pressures, and 2) whether these toxin families exhibit similar patterns across multiple species.

5 | CONCLUSION

We sequenced and assembled the genome of *C. ruber*, characterized range-wide genetic and venom differentiation, and robustly explored the underlying factors associated with venom expression evolution, including neutral evolutionary processes. Venom variation was most significantly and overwhelmingly predicted by snake size; variation across life history may be the result of selection due to differences in prey and/or optimal foraging strategies (Adriaens *et al.*, 2001; Hintz and Lonzarich, 2018) or neutral mechanisms such as developmental constraints (Barton and Boege, 2017; Fernandez-Lorenzo *et al.*, 1999). Additional information on changes in diet preference across life history, functional data of venom toxicity in these prey, and characterization of the regulatory architecture underlying venom expression differentiation across age classes (e.g., Hogan *et al.*, 2024) is needed to further explore the ultimate and proximate mechanisms driving ontogenetic venom variation in *C. ruber*. Although we also found that venom variation was significantly associated with abiotic and biotic factors, neutral patterns explained some variation in the venom phenotype and minimally warrant consideration and inclusion in future models.

By incorporating proxies for neutral and adaptive processes into a singular statistical framework, our study robustly shows the pivotal role of adaptive evolution in snake venoms, consistent with decades of research (Mason *et al.*, 2022; Margres *et al.*, 2017a; Rao *et al.*, 2022; Arbuckle, 2020; Smith *et al.*, 2023; Davies and Arbuckle, 2019; Cipriani *et al.*, 2017; Barlow *et al.*, 2009; Smiley-Walters *et al.*, 2017; Sanz *et al.*, 2006; Sasa, 1999; Margres *et al.*, 2021b; Strickland *et al.*, 2018; Siqueira-Silva *et al.*, 2021; Holding *et al.*, 2018, 2021; Mackessy *et al.*, 2003; Schonour *et al.*, 2020; Holding *et al.*, 2016; Daltry *et al.*, 1996; Casewell *et al.*, 2020; Vonk *et al.*, 2013; Schield *et al.*, 2022). However, several of these previous studies did not adequately account for neutral processes, providing reduced confidence in adaptive interpretations. We acknowledge that our findings are based on the analysis of a single species and trait, and neutral processes may play a larger role in shaping phenotypic variation in other species and biological traits crucial to fitness and survival (Nei, 2005; Ho *et al.*, 2017; Wright, 1931). Consequently, accounting for the influence of neutral evolutionary processes remains critical when investigating the forces producing trait variation, particularly within species. Our findings, together with those of others (e.g., Hague *et al.*, 2020; Aird *et al.*, 2017), underscore the necessity of considering the complexity of evolutionary processes when investigating phenotypic evolution.

6 | MATERIALS AND METHODS

6.1 | Sampling

We collected 21 *C. ruber* across the Baja California Peninsula, MX and southern California, USA (Figure 1). Snakes were captured via road cruising or visual encounter surveys. Upon capture, sampling locality, snout-vent-length (SVL), tail length, and sex were recorded. Venom and blood were sampled in the field from two individuals prior to release. Nineteen individuals were euthanized, dissected, vouchered, and deposited at La Colección Herpetologica de la Facultad de Ciencias Biologicas de la Universidad Juárez del Estado de Durango in Gómez Palacio, Durango, MX. For dissection, we removed the right and left venom glands, heart, liver, gonad, kidney, muscle, and/or blood and stored each tissue in RNALater and/or 95% ethanol. Snakes were collected under the following permits: Secretaría de Medio Ambiente y Recursos Naturales Oficio N SGPA/DGVS/01090/17; SGPA/DGVS/002288/18; SGPA/DGVS/13338/19; SGPA/DGVS/2190/19; SGPA/DGVS/08831/20; SGPA/DGVS/10362/21 and California Department of Fish and Wildlife SC-12985. The procedures outlined were approved by the University of South Florida Institutional Animal Care and Use Committee (IACUC) under protocol IS00011949 and Clemson University IACUC protocol 2017-067.

6.2 | Reference Genome Sequencing and Assembly

A high-quality reference genome for *C. ruber* was produced from a subadult male (66.5 cm SVL, 71.0 cm TL) sampled near Bahía de los Ángeles, Baja California, MX (Figure 1). High-molecular-weight (HMW) genomic DNA (gDNA) was obtained from blood extracted from the caudal vein. The genome was sequenced using Pacific Biosciences HiFi sequencing on 1.5 cells on the Sequel II sequencer at the University of Delaware Sequencing & Genotyping Center. We used HiFiAdapterFilt (Sim *et al.*, 2022) to detect adapter contamination in the sequenced reads and found 1,259 reads (0.00094% of total) with adapters. We assembled the genome using all reads with the Hifiasm assembler (Cheng *et al.*, 2021). We then used Blast (Johnson *et al.*, 2008) with the UniVec database to detect adapters within the assembly and masked all adapter contaminants using the BEDTools maskfasta function (Dale *et al.*, 2011). Assembly quality statistics were calculated using MERQURY (Rhie *et al.*, 2020) and Genome Tools (Gremme *et al.*, 2013). Assembly completeness was assessed using BUSCO (Simão *et al.*, 2015) for datasets Vertebrata and Sauropsida. We screened for foreign contamination of the assembled genome using NCBI FCS-GX (Astashyn *et al.*, 2024; Bush *et al.*, 2024; Pozo *et al.*, 2024). No contamination was detected in the genome assembly and classification of all contigs was consistent with the expected taxonomic composition of the target organism. To achieve a chromosomal representation of the assembly, we aligned the *C. ruber* genome to the *Crotalus adamanteus* genome (Hogan *et al.*, 2024) using Ragtag (Alonge *et al.*, 2022). A Circos plot of the genome was generated using the Circlize package (Gu *et al.*, 2014) in R. Genome assembly and all data generated in this study are available at NCBI PRJNA1051499.

6.3 | Reference Genome Annotation

To aid in genome annotation, we generated transcriptomes for blood, gonad, heart, kidney, liver, and right and left venom glands from the same subadult male used for reference genome assembly (see below for details on RNA extraction and sequencing); all RNA-seq data were aligned to the genome using Hisat2 (Kim *et al.*, 2019). The genome was then annotated using GeMoMa (Keilwagen *et al.*, 2019) with the *Crotalus adamanteus* (Hogan *et al.*, 2024) genome and the aligned *C. ruber* transcriptome data as references. Functional annotations were added using InterProScan (Jones *et al.*, 2014) and Blast (Johnson *et al.*, 2008). Due to the complex architecture of venom genes in large-tandem arrays, automated annotation of venom genes is often unreliable. As such, we used Geneious Prime (Kearse *et al.*, 2012) and FGENESH+ (Salamov and Solovyev, 2000) to manually identify and annotate venom genes as previously described (Margres *et al.*, 2021a).

6.4 | ddRADseq Data Processing

We downloaded double digest restriction-site associated DNA (ddRADseq) data for 34 *C. ruber* from NCBI SRA (Figure 1; PRJNA413434; Harrington *et al.*, 2018). Non-reference based population genomic analyses can be prone to errors arising from repetitive regions, polymorphisms, and sequencing errors (Brandies *et al.*, 2019); therefore, we reanalyzed the *C. ruber* ddRADseq data using reference-based alignment to the generated reference genome described above. All ddRADseq data were aligned to the reference genome using iPγRAD (Eaton and Overcast, 2020) using default parameters.

6.5 | Whole-Genome Sequencing Data Generation and Processing

We generated short-read whole-genome sequencing (WGS) data for six *C. ruber* (PRJNA1051499) and downloaded an additional *C. ruber* whole-genome from NCBI SRA (PRJNA593834; Schield *et al.*, 2022). For the six genomes generated in this study, DNA was isolated from blood samples using the EZNA Tissue DNA Kit (Omega Bio-tek), and DNA libraries were generated using the Ultra II FS DNA Library Prep kit (New England Biolabs). Libraries were sequenced at the North Carolina State University Genomic Sciences Laboratory using Illumina Novaseq 6000 with 150 paired-end sequencing (Supporting Information Table S6). Data were mapped to the reference genome using bowtie2 (Langmead and Salzberg, 2012), and SNPs were called using GATK (McKenna *et al.*, 2010) best practices workflow for germline short variant discovery with default parameters and recommended hard filters. A merged VCF file with the 34 ddRADseq samples and seven WGS samples was produced using bcftools merge and was subsequently filtered using

[396] VCFtools (Danecek *et al.*, 2011) with the following parameters: minimum allele frequency (maf) 0.05, minimum depth (minDP) 5, and
[397] max-missing 0.5. The final combined genomic dataset included 41 individuals and 5,284 SNPs.

6.6 | Transcriptome Sequencing

[399] We sequenced venom-gland transcriptomes from 12 individuals and additional blood, gonad, heart, kidney, and liver transcriptomes
[400] for the reference genome animal (PRJNA1051499) as outlined above. We also downloaded six additional venom-gland transcriptomes
[401] from NCBI SRA (PRJNA88989; Holding *et al.*, 2021). Venom glands were processed following the approach of Rokyta *et al.* (2012).
[402] Briefly, for venom glands, venom was extracted four days prior to euthanasia to allow maximum transcription upon venom gland
[403] extraction (Rotenberg *et al.*, 1971). At four days, snakes were euthanized and dissected. For dissection, the left and right venom
[404] glands, heart, blood, muscle, kidney, liver, and gonad were removed and placed in RNALater. We extracted RNA from the left and
[405] right venom glands separately, then combined in equal quantities for RNA library prep for each snake. For the reference genome
[406] snake, we also extracted RNA from each of the tissues listed above. We isolated RNA using a TRIzol extraction method as outlined
[407] in Rokyta *et al.* (2017). RNA libraries were generated using the Ultra II RNA Library Prep Kit for Illumina (New England Biolabs)
[408] and sequenced at the Florida State University DNA Sequencing Facility using NovaSeq 6000 and the Oklahoma Medical Research
[409] Foundation Clinical Genomics Center using the NovaSeq X Plus with 150 paired-end sequencing (Supporting Information Table S6).
[410] Because gene expression values are sensitive to the read count methods employed, particularly for genes with exceptionally low and
[411] high expression (Liu *et al.*, 2022), we mapped each transcriptome to the generated reference genome using Hisat2 (Kim *et al.*, 2019)
[412] and estimated read counts for genes using both HTSeq-count (Anders *et al.*, 2015; Putri *et al.*, 2022) and Stringtie2 (Pertea *et al.*, 2015).
[413] We used these two read-count estimation methods to provide complementary yet distinct quantitative estimates of gene expression
[414] to account for potential biases inherent in each approach. StringTie2 assembles RNA transcripts and estimates gene expression based
[415] on these assembled transcripts. HTSeq-counts directly counts the number of reads mapped to predefined features (e.g., genes labeled
[416] in a GFF3 annotation file), providing a direct measure of gene expression but potentially overlooking transcript complexity, such as
[417] alternative splicing or multiple isoforms, which may be better accounted for by StringTie2.

6.7 | Estimating Population Structure and Neutral Genetic Divergence

[419] To recharacterize *C. ruber* population structure (Harrington *et al.*, 2018), we used conStruct (Bradburd *et al.*, 2018) on the combined
[420] genomic dataset ($n = 41$) described above. We removed SNPs with >30% missing data and subsequently removed two individuals
[421] with >50% missing data for a reduced dataset containing 39 individuals and 2,241 SNPs. We initially tested $K = 1-5$ genetic clusters
[422] using both spatial and non-spatial models and compared predictive accuracies using cross-validation. For each value of K and each
[423] type of model, we ran cross-validation using 20 replicates and 10,000 iterations, with SNPs split into 75% training and 25% testing
[424] data partitions. We ran each model for 20,000 iterations using three independent MCMC replicates. Additionally, we investigated
[425] patterns of sequence dissimilarity across all individuals and SNPS ($n = 41$; 5,284 SNPs) using principal coordinate analysis (PCoA) from
[426] the R package dartR (Gruber *et al.*, 2018). We then calculated F_{ST} between the defined populations using VCFtools (Danecek *et al.*,
[427] 2011) on both the full (n = 41; 5,284 SNPs) and reduced (n = 39; 2,241 SNPs) genomic dataset.

6.8 | Estimating Effective Migration Surfaces

[429] To infer migration rates in *C. ruber*, we used EEMS (Petkova *et al.*, 2016) on the full combined genomic dataset (n = 41; 5,284 SNPs). We
[430] converted the merged WGS and ddRADseq SNP dataset to PLINK format (Purcell *et al.*, 2007) and transformed the data to a pairwise
[431] distance matrix using "bed2diffs" function in EEMS. We used EEMS to estimate migration surfaces by running three independent
[432] chains, each with 1,000 demes, 10,000,000 MCMC iterations, 1,000,000 iterations of burn-in, and a thinning interval of 10,000. All
[433] chains successfully converged (Supporting Information Figure S5).

6.9 | Estimating Demographic History

[435] To estimate effective population size (N_e) through time for each *C. ruber* population as identified in conStruct above, we used pairwise
[436] sequentially Markovian coalescence (PSMC; Li and Durbin, 2011). We used PSMC over similar methods (e.g., MSMC, SMC++, Stairway
[437] Plot; Schiffels and Durbin, 2014; Terhorst *et al.*, 2017; Liu and Fu, 2015) due to its higher precision and accuracy, especially during
[438] intermediate (~10,000 – 666 generations) time periods (Patton *et al.*, 2019); however, PSMC may imprecisely estimate N_e towards the
[439] present (Liu and Fu, 2015; Patton *et al.*, 2019; Nadachowska-Brzyska *et al.*, 2016). Therefore, interpretations of historical demographic
[440] history based on our analyses were limited to intermediate evolutionary timescales as defined above. We inferred N_e across 28 free
[441] atomic time intervals (4+25*2+4+6) and checked for variance in N_e estimation by performing 100 bootstrap replicates (Supporting
[442] Information Figure S6). We used the published generation time (g = 3.3) and mutation rate ($\mu = 0.7 \; x \; 10^{-8}$) of sister taxon *Crotalus*
[443] *atrox* (Castoe *et al.*, 2007; Holding *et al.*, 2021).

6.10 | Venom Proteomics

To characterize *C. ruber* venom variation, we collected venom from 20 individuals and used reversed-phase high performance liquid chromatography (RP-HPLC) to quantify venom protein expression. Venom was collected and then dried and stored at -80°C prior to analysis. We conducted RP-HPLC on a Dionex ultimate 3000 UHPLC DAD (Thermo Fisher Scientific) and a BeckmanSystem Gold HPLC (BeckmanCoulter) using a Jupiter® 5 μm C18 300 Å, LC Column 250 x 2 mm, Ea column. 50 μg of total venom protein were injected onto the column using a solvent system of A = 0.1% trifluoroacetic acid (TFA) in water and B = 0.075% TFA in acetonitrile. After five minutes at 5% B, a 1% per minute linear gradient of A and B was run to 25% B, followed by a 0.25% per minute gradient from 25% to 65% B at a flow rate of 0.6 mL per min (Margres *et al.*, 2014). Column effluent was monitored at 220 nm. RP-HPLC peaks were quantified in the Chromeleon^{TM} software (Thermo Fisher Scientific). To estimate the relative abundance of each protein peak, we measured the area under the peak relative to the total area of all peaks identified (Gibbs and Rossiter, 2008). Prior to statistical analyses, quantified peaks were transformed in R using isometric Log-Ratio (ILR) from the rombCompositions package (Templ *et al.*, 2023).

6.11 | Characterizing Venom Expression Differentiation

To identify patterns of venom expression variation, we first conducted a PCA on the ILR transformed venom proteomic data (*n* = 20) in R using the "prcomp" function from the Stats package. We then conducted a simple regression model ("lm" function in R) comparing PC1 with SVL to test for the effects of ontogeny, which is common in rattlesnakes (Durban *et al.*, 2017; Margres *et al.*, 2015a,b; Wray *et al.*, 2015; Rokyta *et al.*, 2017; Schonour *et al.*, 2020; Barlow *et al.*, 2009; Borja *et al.*, 2018; Andrade and Abe, 1999; Cipriani *et al.*, 2017; Modahl *et al.*, 2016; Alape-Girón *et al.*, 2008). To determine whether venom protein expression was significantly different across populations and/or age classes, we performed a permutational multivariate analysis of variance (PERMANOVA) in the "adonis2" function of the vegan package (Oksanen *et al.*, 2020) on the ILR transformed venom proteomic data. The same approach using PCA, simple regression, and PERMANOVA was repeated using normalized venom-gland transcriptomic data from HTSeq-count (*n* = 18; Anders *et al.*, 2015; Putri *et al.*, 2022) to verify concordance between venom proteomic and venom-gland transcriptomic data. Read count data from HTSeq-count were normalized using median of ratios from DEseq2 (Anders and Huber, 2010).

We also tested whether specific toxin transcripts were significantly differentially expressed (DE) across populations and/or age classes using the program DESeq2 (Love *et al.*, 2014) on our venom-gland transcriptome data (*n = 18*). For the geographic comparison, we used the two populations as delineated from conStruct (Bradburd *et al.*, 2018) and accounted for ontogeny in the model by using age class as a covariate. For the ontogenetic comparison, we accounted for geography in the model by including population as a covariate. Significance in differential expression was calculated using the FDR-adjusted p value (padj) and log2 fold change (LFC) $\geq$ 1 from DESeq2.

6.12 | Determining the Contributions of Ecological and Evolutionary Factors on Venom Expression Variation through Conditional Redundancy Analysis

To estimate the contributions of neutral processes, life history (i.e., snake size), prey availability and diversity, and climactic conditions on *C. ruber* venom expression variation, we used conditional Redundancy Analyses (RDA; van den Wollenberg, 1977; Capblancq and Forester, 2021; Liu, 1997). Briefly, conditional RDA controls for the effects of one set of explanatory variables prior to conducting RDA on the residual matrix. RDA functions as an extension to multiple regression analysis but permits multivariate response variables. Significance testing within an RDA framework utilizes permutation, making it robust to small sample size and distributional assumptions (Liu, 1997).

Here, we explored venom expression variation using eight different response variables: (1) estimated read counts for all toxin genes using HTSeq-counts (Anders *et al.*, 2015; Putri *et al.*, 2022), (2) estimated read counts for all toxin genes using Stringtie2 (Pertea *et al.*, 2015) and (3–8) estimated read counts for specific paralogs belonging to the six dominant toxin families individually using HTSeq-counts. All venom response variables were multivariate toxin gene expression data representing the abundance levels of multiple toxin loci, enabling us to identify the most significant explanatory variables influencing the expression of toxin genes within a multivariate framework. Prior to analysis, we transformed read count data using the median of ratios in DESeq2 (Anders and Huber, 2010). We conditioned each explanatory variable (nontoxin sequence variation, toxin sequence variation, climactic variation, prey availability, and prey diversity, each described below) in the model on the other explanatory variables to remove the potential confounding effects for each. We then conducted a marginal test using all explanatory variables and used forward model selection to generate the marginal model (i.e., best model). Conditional RDAs were conducted using the "rda" function from the Vegan package in R (Oksanen *et al.*, 2020) and included the "anova" function for significance testing, "RsquareAdj" for model fit, and "ordiR2step" for forward model selection. We describe each explanatory variable below:

1) To include the contributions of neutral processes in the model, we generated a SNP dataset for nontoxin genes, our proxy for neutrality (Holding *et al.*, 2021; Rautsaw *et al.*, 2019), sequenced from the venom-gland transcriptomes (*n* = 18). We used GATK (McKenna *et al.*, 2010) with default parameters as previously outlined. Additional filtering parameters from VCFtools (Danecek *et al.*, 2011) included min-alleles 2, minDP 5, max-missing 0.5, and minimum allele frequency of 0.1. We converted our annotated reference genome file to a BED file and used VCFTools with functions "bed" and "exclude-bed" to isolate nontoxin genes from toxin genes, resulting in 41,236 nontoxin SNPS for analysis. We also attempted to remove potential signatures of selection from the nontoxin SNP data by creating a second dataset containing only synonymous sites. Variant annotation was conducted using SnpEff (Cingolani

et al., 2012), resulting in 3,818 nontoxin synonymous SNPs. Nontoxin sequence variation was summarized using principal Coordinate Analysis (PCoA) from the R package dartR (Gruber *et al.*, 2018) on both the full nontoxin SNP dataset (41,236 SNPs) and the nontoxin synonymous SNP dataset (3,818 SNPs; Supporting Information Figure S2B-C). To determine whether the inclusion of other nontoxin SNP types (nonsynonmous and intronic) accurately represented neutral genetic divergence, we conducted a regression using PCo1 of the full nontoxin SNP dataset and PCo1 of the nontoxin synonymous SNP dataset (Supporting Information Figure S4). We retained PCo1 and PCo2 of the full nontoxin SNP dataset (41,236 SNPs) for use in the conditional RDAs (Supporting Information Table S7).

2) To include signatures of selection on toxin gene sequences, we summarized toxin sequence variation from venom gland transcriptomes (*n* = 18) following the same approach above; however, following filtration, toxin genes were isolated from nontoxin genes, resulting in a toxin-only SNP dataset of 1,760 SNPs. Note that toxin sequence variation was excluded as a variable in individual toxin families due to to the limited number of independent SNPs for each family (Supporting Information Figure S2D and Table S7).

3) Abiotic factors were incorporated using differing environmental conditions as represented by the 19 Worldclim Bioclim variables (Hijmans *et al.*, 2005) at each sampling site using 5 minute spatial resolution. We conducted a PCA across the data, and PC1 and PC2 were retained for use in the conditional RDAs (See Supporting Information Table S4 for PC loadings and proportion of variance explained by each PC).

4) To account for potential differences in diet between individuals, we incorporated prey availability in the model following the approach of Holding *et al.* (2018). Prey availability was determined using published accounts of prey data for *C. ruber* (Dugan and Hayes, 2012; Clark *et al.*, 2012; Klauber, 1997; Holding *et al.*, 2021) resulting in 29 known prey items (Supporting Information Table S5). Geographic range was determined for each prey item using iNaturalist (www.inaturalist.org), IUCN (www.iucn.org), and/or Map of Life (mol.org). For each sample site, each prey item was given a value of "1" if present and "0" if absent (Supporting Information Table S7). We conducted Non-metric multi-dimensional scaling (NMDS) on the prey dataset using the "metaMDS" function from the Vegan package in R (Oksanen *et al.*, 2020) and retained MDS1 and MDS2 for use in the conditional RDAs (See Supporting Information Table S5 for NMDS loadings and proportion of variance explained by each MDS).

5) Phylogenetic diversity of prey has been shown to predict patterns of venom evolution across species (Holding *et al.*, 2021); therefore, we incorporated estimates of prey mean phylogenetic distance (MPD) in the model. We generated a phylogeny of the 29 *C. ruber* prey items using www.timetree.org (Supporting Information Figure S7; Kumar *et al.*, 2017) and used the "ses.mpd" function from the Picante R package (Kembel *et al.*, 2010) to calculate MPD at each site (Supporting Information Table S8).

See Supporting Information Table S7 for data used in conditional RDAs.

7 | AUTHOR CONTRIBUTIONS

S.R.H. and M.J.M. conceived and designed the study. All authors contributed to data collection and/or generation. S.R.H. and M.A.B. analyzed data. S.R.H. led writing with input from all coauthors.

8 | FUNDING INFORMATION

9 | ACKNOWLEDGMENTS

10 | DATA AVAILABILITY

The data underlying this article are available in its online supplementary material and the National Center for Biotechnology Information (NCBI). All sequencing data generated in the study were submitted to NCBI under BioProject (PRJNA1051499). Accession numbers can be found in Supporting Information Table S6. Metadata are provided in Supporting Information Tables S1, S6, and S7. Ecological data were obtained from publicly available databases and all analytical softwares are publicly available.

11 | CONFLICT OF INTEREST

The authors declare no conflicts of interest.

references

Adriaens, D., Aerts, P., and Verraes, W. 2001. Ontogenetic shift in mouth opening mechanisms in a catfish (Clariidae, Siluriformes): A response to increasing functional demands. *J Morph*, 247(3): 197–216.

Aird, S. D., Arora, J., Barua, A., Qiu, L., Terada, K., and Mikheyev, A. S. 2017. Population Genomic Analysis of a Pitviper Reveals Microevolutionary Forces Underlying Venom Chemistry. *Genome Biol Evol*, 9(10): 2640–2649.

Alape-Girón, A., Sanz, L., Escolano, J., Flores-Díaz, M., Madrigal, M., Sasa, M., and Calvete, J. J. 2008. Snake Venomics of the Lancehead Pitviper Bothrops asper: Geographic, Individual, and Ontogenetic Variations. *J Proteome Res*, 7(8): 3556–3571.

Alencar, L. R. V., Quental, T. B., Grazziotin, F. G., Alfaro, M. L., Martins, M., Venzon, M., and Zaher, H. 2016. Diversification in vipers: Phylogenetic relationships, time of divergence and shifts in speciation rates. *Mol Phylogenet Evol*, 105: 50–62.

Alexander, H. J., Taylor, J. S., Wu, S. S.-T., and Breden, F. 2006. Parallel Evolution and Vicariance in the Guppy (poecilia Reticulata) Over Multiple Spatial and Temporal Scales. *Evolution*, 60(11): 2352–2369.

Alonge, M., Lebeigle, L., Kirsche, M., Jenike, K., Ou, S., Aganezov, S., Wang, X., Lippman, Z. B., Schatz, M. C., and Soyk, S. 2022. Automated assembly scaffolding using RagTag elevates a new tomato system for high-throughput genome editing. *Genome Biol*, 23(1): 258.

Anders, S. and Huber, W. 2010. Differential expression analysis for sequence count data. *Genome Biology*, 11(10): R106.

Anders, S., Pyl, P. T., and Huber, W. 2015. HTSeq—a Python framework to work with high-throughput sequencing data. *Bioinformatics*, 31(2): 166–169.

Andrade, D. V. and Abe, A. S. 1999. Relationship of Venom Ontogeny and Diet in Bothrops. *Herpetologica*, 55(2): 200–204.

Arbuckle, K. 2020. From molecules to macroevolution: Venom as a model system for evolutionary biology across levels of life. *Toxicon*, 6: 100034.

Astashyn, A., Tvedte, E. S., Sweeney, D., Sapojnikov, V., Bouk, N., Joukov, V., Mozes, E., Strope, P. K., Sylla, P. M., Wagner, L., et al. 2024. Rapid and sensitive detection of genome contamination at scale with fcs-gx. *Gen Bio*, 25(1): 60.

Barlow, A., Pook, C. E., Harrison, R. A., and Wüster, W. 2009. Coevolution of diet and prey-specific venom activity supports the role of selection in snake venom evolution. *Proc Natl Acad Sci*, 276(1666): 2443–2449.

Barton, K. E. and Boege, K. 2017. Future directions in the ontogeny of plant defence: Understanding the evolutionary causes and consequences. *Ecolo Let*, 20(4): 403–411.

Borja, M., Neri-Castro, E., Pérez-Morales, R., Strickland, J. L., Ponce-López, R., Parkinson, C. L., Espinosa-Femat, J., Sáenz-Mata, J., Flores-Martínez, E., Alagón, A., and Castañeda-Gaytán, G. 2018. Ontogenetic Change in the Venom of Mexican Black-Tailed Rattlesnakes (Crotalus molossus nigrescens). *Toxins*, 10(12): 501.

Bradburd, G. S., Coop, G. M., and Ralph, P. L. 2018. Inferring Continuous and Discrete Population Genetic Structure Across Space. *Genetics*, 210(1): 33–52.

Brandies, P., Peel, E., Hogg, C. J., and Belov, K. 2019. The Value of Reference Genomes in the Conservation of Threatened Species. *Genes*, 10(11): 846.

Brenes, F., Gutiérrez, J. M., and Lomonte, B. 1987. Immunohistochemical demonstration of the binding of Bothrops asper myotoxin to skeletal muscle sarcolemma. *Toxicon*, 25(5): 574–577.

Brodie, E. D. and Brodie, E. D. 1990. Tetrodotoxin Resistance in Garter Snakes: An Evolutionary Response of Predators to Dangerous Prey. *Evolution*, 44(3): 651–659.

Brodie, E. D., Ridenhour, B. J., and Brodie, E. D. 2002. The evolutionary response of predators to dangerous prey: Hotspots and coldspots in the geographic mosaic of coevolution between garter snakes and newts. *Evolution*, 56(10): 2067–2082.

Brodie, E. D., Feldman, C. R., Hanifin, C. T., Motychak, J. E., Mulcahy, D. G., Williams, B. L., and Brodie, E. D. 2005. Parallel Arms Races between Garter Snakes and Newts Involving Tetrodotoxin as the Phenotypic Interface of Coevolution. *J Chem Ecol*, 31(2): 343–356.

Broecker, W. S. and Hemming, S. 2001. Climate Swings Come into Focus. *Science*, 294(5550): 2308–2309.

Brown, S. K., Hull, J. M., Updike, D. R., Fain, S. R., and Ernest, H. B. 2009. Black Bear Population Genetics in California: Signatures of Population Structure, Competitive Release, and Historical Translocation. *J Mammalogy*, 90(5): 1066–1074.

Bush, J., Webster, C., Wegrzyn, J., Simon, C., Wilcox, E., Khan, R., Weisz, D., Dudchenko, O., Aiden, E. L., and Frandsen, P. 2024. Chromosome-level genome assembly and annotation of a periodical cicada species: Magicicada septendecula. *Gen Bio Evo*, 16(1): evae001.

Capblancq, T. and Forester, B. R. 2021. Redundancy analysis: A Swiss Army Knife for landscape genomics. *Methods Ecol. Evol.*, 12(12): 2298–2309.

Casewell, N. R., Wagstaff, S. C., Harrison, R. A., Renjifo, C., and Wüster, W. 2011. Domain loss facilitates accelerated evolution and neofunctionalization of duplicate snake venom metalloproteinase toxin genes. *Mol Biol Evol*, 28(9): 2637–2649.

Casewell, N. R., Wagstaff, S. C., Wüster, W., Cook, D. A. N., Bolton, F. M. S., King, S. I., Pla, D., Sanz, L., Calvete, J. J., and Harrison, R. A. 2014. Medically important differences in snake venom composition are dictated by distinct postgenomic mechanisms. *Proc Natl Acad Sci*, 111(25): 9205–9210.

Casewell, N. R., Jackson, T. N. W., Laustsen, A. H., and Sunagar, K. 2020. Causes and Consequences of Snake Venom Variation. *Trends in Pharm Sci*, 41(8): 570–581.

Castoe, T. A., Spencer, C. L., and Parkinson, C. L. 2007. Phylogeographic structure and historical demography of the western diamondback rattlesnake (Crotalus atrox): A perspective on North American desert biogeography. *Mol Phylogenet Evol*, 42(1): 193–212.

Cheng, H., Concepcion, G. T., Feng, X., Zhang, H., and Li, H. 2021. Haplotype-resolved de novo assembly using phased assembly graphs with hifiasm. *Nat Methods*, 18(2): 170–175.

Cingolani, P., Platts, A., Wang, L. L., Coon, M., Nguyen, T., Wang, L., Land, S. J., Lu, X., and Ruden, D. M. 2012. A program for annotating and predicting the effects of single nucleotide polymorphisms, SnpEff. *Fly (Austin)*, 6(2): 80–92.

Cipriani, V., Debono, J., Goldenberg, J., Jackson, T. N. W., Arbuckle, K., Dobson, J., Koludarov, I., Li, B., Hay, C., Dunstan, N., Allen, L., Hendrikx, I., Kwok, H. F., and Fry, B. G. 2017. Correlation between ontogenetic dietary shifts and venom variation in Australian brown snakes (Pseudonaja). *Comp Biochem Physiol*, 197: 53–60.

Clark, R. W., Tangco, S., and Barbour, M. A. 2012. Field video recordings reveal factors influencing predatory strike success of free-ranging rattlesnakes (Crotalus spp.). *Anim Behav*, 84(1): 183–190.

Dale, R. K., Pedersen, B. S., and Quinlan, A. R. 2011. Pybedtools: A flexible Python library for manipulating genomic datasets and annotations. *Bioinformatics*, 27(24): 3423–3424.

Daltry, J. C., Wüster, W., and Thorpe, R. S. 1996. Diet and snake venom evolution. *Nature*, 379(6565): 537–540.

Danecek, P., Auton, A., Abecasis, G., Albers, C. A., Banks, E., DePristo, M. A., Handsaker, R. E., Lunter, G., Marth, G. T., Sherry, S. T., McVean, G., Durbin, R., and 1000 Genomes Project Analysis Group 2011. The variant call format and VCFtools. *Bioinformatics*, 27(15): 2156–2158.

Darwin, C. 1859. *On the Origin of Species by Means of Natural Selection, Or The Preservation of Favoured Races in the Struggle for Life*. John Murray, Albemarle Street.

Davies, E.-L. and Arbuckle, K. 2019. Coevolution of Snake Venom Toxic Activities and Diet: Evidence that Ecological Generalism Favours Toxicological Diversity. *Toxins*, 11(12): 711.

Dickson, L. B., Jiolle, D., Minard, G., Moltini-Conclois, I., Volant, S., Ghozlane, A., Bouchier, C., Ayala, D., Paupy, C., Moro, C. V., and Lambrechts, L. 2017. Carryover effects of larval exposure to different environmental bacteria drive adult trait variation in a mosquito vector. *Sci Adv*, 3(8): e1700585.

Dolby, G. A., Bennett, S. E., Dorsey, R. J., Stokes, M. F., Riddle, B. R., Lira-Noriega, A., Munguia-Vega, A., and Wilder, B. T. 2022. Integrating Earth–life systems: A geogenomic approach. *Trends Ecol Evol*, 37(4): 371–384.

Dugan, E. A. and Hayes, W. K. 2012. Diet and Feeding Ecology of the Red Diamond Rattlesnake, Crotalus Ruber (serpentes: Viperidae). *Herpetologica*, 68(2): 203–217.

Durban, J., Sanz, L., Trevisan-Silva, D., Neri-Castro, E., Alagón, A., and Calvete, J. J. 2017. Integrated Venomics and Venom Gland Transcriptome Analysis of Juvenile and Adult Mexican Rattlesnakes Crotalus simus, C. tzabcan, and C. culminatus Revealed miRNA-modulated Ontogenetic Shifts. *J Proteome Res*, 16(9): 3370–3390.

Eaton, D. A. R. and Overcast, I. 2020. Ipyrad: Interactive assembly and analysis of RADseq datasets. *Bioinformatics*, 36(8): 2592–2594.

Ernest, H. B., Boyce, W. M., Bleich, V. C., May, B., Stiver, S. J., and Torres, S. G. 2003. Genetic structure of mountain lion (Puma concolor) populations in California. *Cons Gen*, 4(3): 353–366.

Fernandez-Lorenzo, J. L., Rigueiro, A., and Ballester, A. 1999. Polyphenols as potential markers to differentiate juvenile and mature chestnut shoot cultures. *Tree Physiol*, 19(7): 461–466.

Fisher, R. A. 1930. 086: The Distribution of Gene Ratios for Rare Mutations.

Fraser, H. B. 2013. Gene expression drives local adaptation in humans. *Genome Res.*, 23(7): 1089–1096.

Garant, D., Forde, S. E., and Hendry, A. P. 2007. The multifarious effects of dispersal and gene flow on contemporary adaptation. *Func Ecol*, 21(3): 434–443.

Gibbs, H. L. and Mackessy, S. P. 2009. Functional basis of a molecular adaptation: Prey-specific toxic effects of venom from Sistrurus rattlesnakes. *Toxicon*, 53(6): 672–679.

Gibbs, H. L. and Rossiter, W. 2008. Rapid Evolution by Positive Selection and Gene Gain and Loss: PLA2 Venom Genes in Closely Related Sistrurus Rattlesnakes with Divergent Diets. *J Mol Evol*, 66(2): 151–166.

Gibbs, H. L., Prior, K. A., Weatherhead, P. J., and Johnson, G. 1997. Genetic structure of populations of the threatened eastern massasauga rattlesnake, Sistrurus c. catenatus: Evidence from microsatellite DNA markers. *Mol Ecol*, 6(12): 1123–1132.

Gibbs, H. L., Sanz, L., and Calvete, J. J. 2009. Snake population venomics: Proteomics-based analyses of individual variation reveals significant gene regulation effects on venom protein expression in Sistrurus rattlesnakes. *J Mol Evol*, 68(2): 113–125.

Gibbs, H. L., Sanz, L., Chiucchi, J. E., Farrell, T. M., and Calvete, J. J. 2011. Proteomic analysis of ontogenetic and diet-related changes in venom composition of juvenile and adult Dusky Pigmy rattlesnakes (Sistrurus miliarius barbouri). *J Proteomics*, 74(10): 2169–2179.

Gibbs, H. L., Sanz, L., Pérez, A., Ochoa, A., Hassinger, A. T., Holding, M. L., and Calvete, J. J. 2020. The molecular basis of venom resistance in a rattlesnake-squirrel predator-prey system. *Mol Ecol*, 29(15): 2871–2888.

Gompel, N., Prud'homme, B., Wittkopp, P. J., Kassner, V. A., and Carroll, S. B. 2005. Chance caught on the wing: Cis-regulatory evolution and the origin of pigment patterns in Drosophila. *Nature*, 433(7025): 481–487.

Gould, S. J. and Lewontin, R. C. 1979. The Spandrels of San Marco and the Panglossian Paradigm: A Critique of the Adaptationist Programme. *Proc Natl Acad Sci*, 205(1161): 581–598.

Grant, P. R. and Grant, B. R. 2002. Unpredictable Evolution in a 30-Year Study of Darwin's Finches. *Science*, 296(5568): 707–711.

Greenberg, D. B. 2002. *The Ecology of Movement and Site Selection in Desert Rattlesnakes (Crotalus Mitchellii and Crotalus Ruber) of the Southwestern United States*. Ph.D. thesis, University of California, Santa Barbara, United States – California.

Gremme, G., Steinbiss, S., and Kurtz, S. 2013. GenomeTools: A Comprehensive Software Library for Efficient Processing of Structured Genome Annotations. *Transactions Comp Bio Bioinformatics*, 10(3): 645–656.

Grismer, L. L. 2002. *Amphibians and Reptiles of Baja California, Including Its Pacific Islands and the Islands in the Sea of Cortés*. University of California Press.

Gruber, B., Unmack, P. J., Berry, O. F., and Georges, A. 2018. Dartr: An r package to facilitate analysis of SNP data generated from reduced representation genome sequencing. *Mol Ecol Resour*, 18(3): 691–699.

Gu, Z., Gu, L., Eils, R., Schlesner, M., and Brors, B. 2014. Circlize implements and enhances circular visualization in R. *Bioinformatics*, 30(19): 2811–2812.

Hague, M. T. J., Stokes, A. N., Feldman, C. R., Brodie Jr., E. D., and Brodie III, E. D. 2020. The geographic mosaic of arms race coevolution is closely matched to prey population structure. *Evo Letters*, 4(4): 317–332.

Hanifin, C. T., Jr, E. D. B., and Iii, E. D. B. 2008. Phenotypic Mismatches Reveal Escape from Arms-Race Coevolution. *PLOS Bio*, 6(3): e60.

Harrington, S. M., Hollingsworth, B. D., Higham, T. E., and Reeder, T. W. 2018. Pleistocene climatic fluctuations drive isolation and secondary contact in the red diamond rattlesnake (Crotalus ruber) in Baja California. *J Biogeo*, 45(1): 64–75.

Herbert, T. D., Schuffert, J. D., Andreasen, D., Heusser, L., Lyle, M., Mix, A., Ravelo, A. C., Stott, L. D., and Herguera, J. C. 2001. Collapse of the California Current During Glacial Maxima Linked to Climate Change on Land. *Science*, 293(5527): 71–76.

Hester, M. W., Mendelssohn, I. A., and McKee, K. L. 2001. Species and population variation to salinity stress in Panicum hemitomon, Spartina patens, and Spartina alterniflora: Morphological and physiological constraints. *Env Exp Botany*, 46(3): 277–297.

Hijmans, R. J., Cameron, S. E., Parra, J. L., Jones, P. G., and Jarvis, A. 2005. Very high resolution interpolated climate surfaces for global land areas. *Intl J Clim*, 25(15): 1965–1978.

Hintz, W. D. and Lonzarich, D. G. 2018. Maximizing foraging success: The roles of group size, predation risk, competition, and ontogeny. *Ecosphere*, 9(10): e02456.

Ho, W.-C., Ohya, Y., and Zhang, J. 2017. Testing the neutral hypothesis of phenotypic evolution. *Proc Natl Acad Sci*, 114(46): 12219–12224.

Hoekstra, H. E., Hirschmann, R. J., Bundey, R. A., Insel, P. A., and Crossland, J. P. 2006. A Single Amino Acid Mutation Contributes to Adaptive Beach Mouse Color Pattern. *Science*, 313(5783): 101–104.

Hogan, M. P., Holding, M. L., Nystrom, G. S., Colston, T. J., Bartlett, D. A., Mason, A. J., Ellsworth, S. A., Rautsaw, R. M., Lawrence, K. C., Strickland, J. L., He, B., Fraser, P., Margres, M. J., Gilbert, D. M., Gibbs, H. L., Parkinson, C. L., and Rokyta, D. R. 2024. The genetic regulatory architecture and epigenomic basis for age-related changes in rattlesnake venom. *Proc. Natl. Acad. Sci.*, 121(16): e2313440121.

Holding, M. L., Biardi, J. E., and Gibbs, H. L. 2016. Coevolution of venom function and venom resistance in a rattlesnake predator and its squirrel prey. *Proc Royal Soc*, 283(1829): 20152841.

Holding, M. L., Margres, M. J., Rokyta, D. R., and Gibbs, H. L. 2018. Local prey community composition and genetic distance predict venom divergence among populations of the northern Pacific rattlesnake (Crotalus oreganus). *J Evo Bio*, 31(10): 1513–1528.

Holding, M. L., Strickland, J. L., Rautsaw, R. M., Hofmann, E. P., Mason, A. J., Hogan, M. P., Nystrom, G. S., Ellsworth, S. A., Colston, T. J., Borja, M., Castañeda-Gaytán, G., Grünwald, C. I., Jones, J. M., Freitas-de-Sousa, L. A., Viala, V. L., Margres, M. J., Hingst-Zaher, E., Junqueira-de-Azevedo, I. L. M., Moura-da-Silva, A. M., Grazziotin, F. G., Gibbs, H. L., Rokyta, D. R., and Parkinson, C. L. 2021. Phylogenetically diverse diets favor more complex venoms in North American pitvipers. *Proc Natl Acad Sci*, 118(17): e2015579118.

Jackson, T. N. W. and Fry, B. G. 2016. A Tricky Trait: Applying the Fruits of the "Function Debate" in the Philosophy of Biology to the "Venom Debate" in the Science of Toxinology. *Toxins*, 8(9): 263.

Jackson, T. N. W., Koludarov, I., Ali, S. A., Dobson, J., Zdenek, C. N., Dashevsky, D., op den Brouw, B., Masci, P. P., Nouwens, A., Josh, P., Goldenberg, J., Cipriani, V., Hay, C., Hendrikx, I., Dunstan, N., Allen, L., and Fry, B. G. 2016. Rapid Radiations and the Race to Redundancy: An Investigation of the Evolution of Australian Elapid Snake Venoms. *Toxins (Basel)*, 8(11): 309.

Johnson, M., Zaretskaya, I., Raytselis, Y., Merezhuk, Y., McGinnis, S., and Madden, T. L. 2008. NCBI BLAST: A better web interface. *Nuc Acid Res*, 36(suppl_2): W5–W9.

Jones, P., Binns, D., Chang, H.-Y., Fraser, M., Li, W., McAnulla, C., McWilliam, H., Maslen, J., Mitchell, A., Nuka, G., Pesseat, S., Quinn, A. F., Sangrador-Vegas, A., Scheremetjew, M., Yong, S.-Y., Lopez, R., and Hunter, S. 2014. InterProScan 5: Genome-scale protein function classification. *Bioinformatics*, 30(9): 1236–1240.

Juárez, P., Comas, I., González-Candelas, F., and Calvete, J. J. 2008. Evolution of Snake Venom Disintegrins by Positive Darwinian Selection. *Molecular Biology and Evolution*, 25(11): 2391–2407.

Kearse, M., Moir, R., Wilson, A., Stones-Havas, S., Cheung, M., Sturrock, S., Buxton, S., Cooper, A., Markowitz, S., Duran, C., Thierer, T., Ashton, B., Meintjes, P., and Drummond, A. 2012. Geneious Basic: An integrated and extendable desktop software platform for the organization and analysis of sequence data. *Bioinformatics*, 28(12): 1647–1649.

Keilwagen, J., Hartung, F., and Grau, J. 2019. GeMoMa: Homology-Based Gene Prediction Utilizing Intron Position Conservation and RNA-seq Data. In M. Kollmar, editor, *Gene Prediction: Methods and Protocols*, Methods in Molecular Biology, pages 161–177. Springer, New York, NY.

Keller, S. R., Sowell, D. R., Neiman, M., Wolfe, L. M., and Taylor, D. R. 2009. Adaptation and colonization history affect the evolution of clines in two introduced species. *New Phyt*, 183(3): 678–690.

Kembel, S. W., Cowan, P. D., Helmus, M. R., Cornwell, W. K., Morlon, H., Ackerly, D. D., Blomberg, S. P., and Webb, C. O. 2010. Picante: R tools for integrating phylogenies and ecology. *Bioinformatics*, 26(11): 1463–1464.

Kim, D., Paggi, J. M., Park, C., Bennett, C., and Salzberg, S. L. 2019. Graph-based genome alignment and genotyping with HISAT2 and HISAT-genotype. *Nat Biotechnol*, 37(8): 907–915.

Kimura, M. 1968. Evolutionary Rate at the Molecular Level. *Nature*, 217(5129): 624–626.

Kini, R. M. and Koh, C. Y. 2016. Metalloproteases Affecting Blood Coagulation, Fibrinolysis and Platelet Aggregation from Snake Venoms: Definition and Nomenclature of Interaction Sites. *Toxins*, 8(10): 284.

Klauber, L. M. 1997. *Rattlesnakes: Their Habits, Life Histories, and Influence on Mankind*. University of California Press.

Konczal, M., Babik, W., Radwan, J., Sadowska, E. T., and Koteja, P. 2015. Initial Molecular-Level Response to Artificial Selection for Increased Aerobic Metabolism Occurs Primarily through Changes in Gene Expression. *Mol Biol Evol*, 32(6): 1461–1473.

Kumar, S., Stecher, G., Suleski, M., and Hedges, S. B. 2017. TimeTree: A Resource for Timelines, Timetrees, and Divergence Times. *Mol Biol Evol*, 34(7): 1812–1819.

Lande, R. 1976. Natural Selection and Random Genetic Drift in Phenotypic Evolution. *Evolution*, 30(2): 314–334.

Langmead, B. and Salzberg, S. L. 2012. Fast gapped-read alignment with Bowtie 2. *Nat Methods*, 9(4): 357–359.

Li, A., Wang, J., Sun, K., Wang, S., Zhao, X., Wang, T., Xiong, L., Xu, W., Qiu, L., Shang, Y., Liu, R., Wang, S., and Lu, Y. 2021. Two Reference-Quality Sea Snake Genomes Reveal Their Divergent Evolution of Adaptive Traits and Venom Systems. *Mol Biol Evol*, 38(11): 4867–4883.

Li, H. and Durbin, R. 2011. Inference of human population history from individual whole-genome sequences. *Nature*, 475(7357): 493–496.

Liu, Q. 1997. Variation Partitioning by Partial Redundancy Analysis (rda). *Environmetrics*, 8(2): 75–85.

Liu, X. and Fu, Y.-X. 2015. Exploring population size changes using SNP frequency spectra. *Nat Genet*, 47(5): 555–559.

Liu, X., Zhao, J., Xue, L., Zhao, T., Ding, W., Han, Y., and Ye, H. 2022. A comparison of transcriptome analysis methods with reference genome. *BMC Genomics*, 23(1): 232.

Love, M. I., Huber, W., and Anders, S. 2014. Moderated estimation of fold change and dispersion for RNA-seq data with DESeq2. *Genome Biol*, 15(12): 550.

Mackessy, S. P. 1988. Venom Ontogeny in the Pacific Rattlesnakes Crotalus viridis helleri and C. v. oreganus. *Copeia*, 1988(1): 92–101.

Mackessy, S. P. 2021. *Handbook of Venoms and Toxins of Reptiles*. CRC Press.

Mackessy, S. P., Williams, K., and Ashton, K. G. 2003. Ontogenetic Variation in Venom Composition and Diet of Crotalus oreganus concolor: A Case of Venom Paedomorphosis? *Copeia*, 2003(4): 769–782.

Mackessy, S. P., Sixberry, N. M., Heyborne, W. H., and Fritts, T. 2006. Venom of the Brown Treesnake, Boiga irregularis: Ontogenetic shifts and taxa-specific toxicity. *Toxicon*, 47(5): 537–548.

Margres, M. J., Aronow, K., Loyacano, J., and Rokyta, D. R. 2013. The venom-gland transcriptome of the eastern coral snake (Micrurus fulvius) reveals high venom complexity in the intragenomic evolution of venoms. *BMC Genom*, 14(1): 531.

Margres, M. J., McGivern, J. J., Wray, K. P., Seavy, M., Calvin, K., and Rokyta, D. R. 2014. Linking the transcriptome and proteome to characterize the venom of the eastern diamondback rattlesnake (Crotalus adamanteus). *J Proteomics*, 96: 145–158.

Margres, M. J., McGivern, J. J., Seavy, M., Wray, K. P., Facente, J., and Rokyta, D. R. 2015a. Contrasting Modes and Tempos of Venom Expression Evolution in Two Snake Species. *Genetics*, 199(1): 165–176.

Margres, M. J., Wray, K. P., Seavy, M., McGivern, J. J., Sanader, D., and Rokyta, D. R. 2015b. Phenotypic integration in the feeding system of the eastern diamondback rattlesnake (Crotalus adamanteus). *Mol Ecol*, 24(13): 3405–3420.

Margres, M. J., Wray, K. P., Seavy, M., McGivern, J. J., Herrera, N. D., and Rokyta, D. R. 2016a. Expression Differentiation Is Constrained to Low-Expression Proteins over Ecological Timescales. *Genetics*, 202(1): 273–283.

Margres, M. J., Walls, R., Suntravat, M., Lucena, S., Sánchez, E. E., and Rokyta, D. R. 2016b. Functional characterizations of venom phenotypes in the eastern diamondback rattlesnake (Crotalus adamanteus) and evidence for expression-driven divergence in toxic activities among populations. *Toxicon*, 119: 28–38.

Margres, M. J., Wray, K. P., Hassinger, A. T. B., Ward, M. J., McGivern, J. J., Moriarty Lemmon, E., Lemmon, A. R., and Rokyta, D. R. 2017a. Quantity, Not Quality: Rapid Adaptation in a Polygenic Trait Proceeded Exclusively through Expression Differentiation. *Mol Biol Evol*, 34(12): 3099–3110.

Margres, M. J., Bigelow, A. T., Lemmon, E. M., Lemmon, A. R., and Rokyta, D. R. 2017b. Selection To Increase Expression, Not Sequence Diversity, Precedes Gene Family Origin and Expansion in Rattlesnake Venom. *Genetics*, 206(3): 1569–1580.

Margres, M. J., Patton, A., Wray, K. P., Hassinger, A. T. B., Ward, M. J., Lemmon, E. M., Lemmon, A. R., and Rokyta, D. R. 2019. Tipping the Scales: The Migration–Selection Balance Leans toward Selection in Snake Venoms. *Mol Biol Evol*, 36(2): 271–282.

Margres, M. J., Rautsaw, R. M., Strickland, J. L., Mason, A. J., Schramer, T. D., Hofmann, E. P., Stiers, E., Ellsworth, S. A., Nystrom, G. S., Hogan, M. P., Bartlett, D. A., Colston, T. J., Gilbert, D. M., Rokyta, D. R., and Parkinson, C. L. 2021a. The Tiger Rattlesnake genome reveals a complex genotype underlying a simple venom phenotype. *Proc Natl Acad Sci*, 118(4): e2014634118.

Margres, M. J., Wray, K. P., Sanader, D., McDonald, P. J., Trumbull, L. M., Patton, A. H., and Rokyta, D. R. 2021b. Varying Intensities of Introgression Obscure Incipient Venom-Associated Speciation in the Timber Rattlesnake (Crotalus horridus). *Toxins*, 13(11): 782.

Mason, A. J., Margres, M. J., Strickland, J. L., Rokyta, D. R., Sasa, M., and Parkinson, C. L. 2020. Trait differentiation and modular toxin expression in palm-pitvipers. *BMC Genomics*, 21(1): 147.

Mason, A. J., Holding, M. L., Rautsaw, R. M., Rokyta, D. R., Parkinson, C. L., and Gibbs, H. L. 2022. Venom Gene Sequence Diversity and Expression Jointly Shape Diet Adaptation in Pitvipers. *Mol Biol Evol*, 39(4): msac082.

Massey, D. J., Calvete, J. J., Sánchez, E. E., Sanz, L., Richards, K., Curtis, R., and Boesen, K. 2012. Venom variability and envenoming severity outcomes of the Crotalus scutulatus scutulatus (Mojave rattlesnake) from Southern Arizona. *J Proteomics*, 75(9): 2576–2587.

McKenna, A., Hanna, M., Banks, E., Sivachenko, A., Cibulskis, K., Kernytsky, A., Garimella, K., Altshuler, D., Gabriel, S., Daly, M., and DePristo, M. A. 2010. The Genome Analysis Toolkit: A MapReduce framework for analyzing next-generation DNA sequencing data. *Genome Res*, 20(9): 1297–1303.

Modahl, C. M., Mukherjee, A. K., and Mackessy, S. P. 2016. An analysis of venom ontogeny and prey-specific toxicity in the Monocled Cobra (Naja kaouthia). *Toxicon*, 119: 8–20.

Müller, R., Kaj, I., and Mugal, C. F. 2022. A Nearly Neutral Model of Molecular Signatures of Natural Selection after Change in Population Size. *Genome Biol Evol*, 14(5): evac058.

Mushinsky, H. R., Hebrard, J. J., and Vodopich, D. S. 1982. Ontogeny of Water Snake Foraging Ecology. *Ecology*, 63(6): 1624–1629.

Nadachowska-Brzyska, K., Burri, R., Smeds, L., and Ellegren, H. 2016. Psmc analysis of effective population sizes in molecular ecology and its application to black-and-white ficedula flycatchers. *Mol Ecol*, 25(5): 1058–1072.

Nei, M. 2005. Selectionism and Neutralism in Molecular Evolution. *Mol Biol Evol*, 22(12): 2318–2342.

Nevo, E. 1978. Genetic variation in natural populations: Patterns and theory. *Theo Pop Biol*, 13(1): 121–177.

Ohta, T. 1973. Slightly Deleterious Mutant Substitutions in Evolution. *Nature*, 246(5428): 96–98.

Oksanen, J., Blanchet, F. G., Friendly, M., Kindt, R., Legendre, P., McGlinn, D., Minchin, P., O'Hara, RB., Simpson, G., Solymos, P., Stevens, MHH., Szöcs, E., and Wagner, H. 2020. *Vegan Community Ecology Package Version 2.5-7 November 2020*.

Patton, A. H., Margres, M. J., Stahlke, A. R., Hendricks, S., Lewallen, K., Hamede, R. K., Ruiz-Aravena, M., Ryder, O., McCallum, H. I., Jones, M. E., Hohenlohe, P. A., and Storfer, A. 2019. Contemporary Demographic Reconstruction Methods Are Robust to Genome Assembly Quality: A Case Study in Tasmanian Devils. *Mol Biol Evol*, 36(12): 2906–2921.

Pertea, M., Pertea, G. M., Antonescu, C. M., Chang, T.-C., Mendell, J. T., and Salzberg, S. L. 2015. StringTie enables improved reconstruction of a transcriptome from RNA-seq reads. *Nat Biotechnol*, 33(3): 290–295.

Petkova, D., Novembre, J., and Stephens, M. 2016. Visualizing spatial population structure with estimated effective migration surfaces. *Nat Genet*, 48(1): 94–100.

Pla, D., Sanz, L., Quesada-Bernat, S., Villalta, M., Baal, J., Chowdhury, M. A. W., León, G., Gutiérrez, J. M., Kuch, U., and Calvete, J. J. 2019. Phylovenomics of Daboia russelii across the Indian subcontinent. Bioactivities and comparative in vivo neutralization and in vitro third-generation antivenomics of antivenoms against venoms from India, Bangladesh and Sri Lanka. *J Proteomics*, 207: 103443.

Pozas-Ocampo, I. F., Carbajal-Saucedo, A., Gatica-Colima, A. B., Cordero-Tapia, A., and Arnaud-Franco, G. 2020. Toxicological comparison of Crotalus ruber lucasensis venom from different ecoregions of the Baja California Peninsula. *Toxicon*, 187: 111–115.

Pozo, G., Albuja-Quintana, M., Larreátegui, L., Gutiérrez, B., Fuentes, N., Alfonso-Cortés, F., and Torres, M. d. L. 2024. First whole-genome sequence and assembly of the ecuadorian brown-headed spider monkey (ateles fusciceps fusciceps), a critically endangered species, using oxford nanopore technologies. *G3*, 14(3): jkae014.

Purcell, S., Neale, B., Todd-Brown, K., Thomas, L., Ferreira, M. A. R., Bender, D., Maller, J., Sklar, P., de Bakker, P. I. W., Daly, M. J., and Sham, P. C. 2007. PLINK: A Tool Set for Whole-Genome Association and Population-Based Linkage Analyses. *Am J Hum Genet*, 81(3): 559–575.

Putri, G. H., Anders, S., Pyl, P. T., Pimanda, J. E., and Zanini, F. 2022. Analysing high-throughput sequencing data in Python with HTSeq 2.0. *Bioinformatics*, 38(10): 2943–2945.

Rao, W.-q., Kalogeropoulos, K., Allentoft, M. E., Gopalakrishnan, S., Zhao, W.-n., Workman, C. T., Knudsen, C., Jiménez-Mena, B., Seneci, L., Mousavi-Derazmahalleh, M., Jenkins, T. P., Rivera-de-Torre, E., Liu, S.-q., and Laustsen, A. H. 2022. The rise of genomics in snake venom research: Recent advances and future perspectives. *Gigascience*, 11: giac024.

Rautsaw, R. M., Hofmann, E. P., Margres, M. J., Holding, M. L., Strickland, J. L., Mason, A. J., Rokyta, D. R., and Parkinson, C. L. 2019. Intraspecific sequence and gene expression variation contribute little to venom diversity in sidewinder rattlesnakes (Crotalus cerastes). *Proc Natl Acad Sci*, 286(1906): 20190810.

Rhie, A., Walenz, B. P., Koren, S., and Phillippy, A. M. 2020. Merqury: Reference-free quality, completeness, and phasing assessment for genome assemblies. *Genome Biol*, 21(1): 245.

Riddle, B. R., Hafner, D. J., Alexander, L. F., and Jaeger, J. R. 2000. Cryptic vicariance in the historical assembly of a Baja California peninsular desert biota. *Proc Natl Acad Sci*, 97(26): 14438–14443.

Robinson, K. E., Holding, M. L., Whitford, M. D., Saviola, A. J., Yates III, J. R., and Clark, R. W. 2021. Phenotypic and functional variation in venom and venom resistance of two sympatric rattlesnakes and their prey. *J Evo Bio*, 34(9): 1447–1465.

Rohlfs, R. V., Harrigan, P., and Nielsen, R. 2014. Modeling Gene Expression Evolution with an Extended Ornstein–Uhlenbeck Process Accounting for Within-Species Variation. *Mol Biol Evol*, 31(1): 201–211.

Rokyta, D. R., Lemmon, A. R., Margres, M. J., and Aronow, K. 2012. The venom-gland transcriptome of the eastern diamond-back rattlesnake (Crotalus adamanteus). *BMC Genom*, 13(1): 312.

Rokyta, D. R., Wray, K. P., and Margres, M. J. 2013. The genesis of an exceptionally lethal venom in the timber rattlesnake (Crotalus horridus) revealed through comparative venom-gland transcriptomics. *BMC Genomics*, 14(1): 394.

Rokyta, D. R., Margres, M. J., and Calvin, K. 2015. Post-transcriptional Mechanisms Contribute Little to Phenotypic Variation in Snake Venoms. *G3*, 5(11): 2375–2382.

Rokyta, D. R., Margres, M. J., Ward, M. J., and Sanchez, E. E. 2017. The genetics of venom ontogeny in the eastern diamond-back rattlesnake (Crotalus adamanteus). *PeerJ*, 5: e3249.

Rotenberg, D., Bamberger, E. S., and Kochva, E. 1971. Studies on ribonucleic acid synthesis in the venom glands of Vipera palaestinae (Ophidia, Reptilia). *Biochem Journal*, 121(4): 609–612.

Salamov, A. A. and Solovyev, V. V. 2000. Ab initio Gene Finding in Drosophila Genomic DNA. *Genome Res.*, 10(4): 516–522.

Sanz, L., Gibbs, H. L., Mackessy, S. P., and Calvete, J. J. 2006. Venom Proteomes of Closely Related Sistrurus Rattlesnakes with Divergent Diets. *J Proteome Res*, 5(9): 2098–2112.

Sasa, M. 1999. Diet and snake venom evolution: Can local selection alone explain intraspecific venom variation? *Toxicon*, 37(2): 249–252; author reply 253–260.

Schield, D. R., Card, D. C., Hales, N. R., Perry, B. W., Pasquesi, G. M., Blackmon, H., Adams, R. H., Corbin, A. B., Smith, C. F., Ramesh, B., Demuth, J. P., Betrán, E., Tollis, M., Meik, J. M., Mackessy, S. P., and Castoe, T. A. 2019. The origins and evolution of chromosomes, dosage compensation, and mechanisms underlying venom regulation in snakes. *Genome Res*, 29(4): 590–601.

Schield, D. R., Perry, B. W., Adams, R. H., Holding, M. L., Nikolakis, Z. L., Gopalan, S. S., Smith, C. F., Parker, J. M., Meik, J. M., DeGiorgio, M., Mackessy, S. P., and Castoe, T. A. 2022. The roles of balancing selection and recombination in the evolution of rattlesnake venom. *Nat Ecol Evol*, 6(9): 1367–1380.

Schiffels, S. and Durbin, R. 2014. Inferring human population size and separation history from multiple genome sequences. *Nat Genet*, 46(8): 919–925.

Schmidt, D. A. 2019. *Patterns of Population Structure and Genetic Diversity among Western Rattlesnakes (Crotalus Oreganus) in the Pacific Northwest*. Ph.D. thesis, University of British Columbia.

Schonour, R. B., Huff, E. M., Holding, M. L., Claunch, N. M., Ellsworth, S. A., Hogan, M. P., Wray, K., McGivern, J., Margres, M. J., Colston, T. J., and Rokyta, D. R. 2020. Gradual and Discrete Ontogenetic Shifts in Rattlesnake Venom Composition and Assessment of Hormonal and Ecological Correlates. *Toxins*, 12(10): 659.

Senji Laxme, R. R., Khochare, S., de Souza, H. F., Ahuja, B., Suranse, V., Martin, G., Whitaker, R., and Sunagar, K. 2019. Beyond the 'big four': Venom profiling of the medically important yet neglected Indian snakes reveals disturbing antivenom deficiencies. *PLoS Negl Trop Dis*, 13(12): e0007899.

Serra, F., Becher, V., and Dopazo, H. 2013. Neutral Theory Predicts the Relative Abundance and Diversity of Genetic Elements in a Broad Array of Eukaryotic Genomes. *PLOS ONE*, 8(6): e63915.

Shine, R. 1991. Why do Larger Snakes Eat Larger Prey Items? *Func Ecol*, 5(4): 493–502.

Sim, S. B., Corpuz, R. L., Simmonds, T. J., and Geib, S. M. 2022. HiFiAdapterFilt, a memory efficient read processing pipeline, prevents occurrence of adapter sequence in PacBio HiFi reads and their negative impacts on genome assembly. *BMC Genomics*, 23(1): 157.

Simão, F. A., Waterhouse, R. M., Ioannidis, P., Kriventseva, E. V., and Zdobnov, E. M. 2015. BUSCO: Assessing genome assembly and annotation completeness with single-copy orthologs. *Bioinformatics*, 31(19): 3210–3212.

Siqueira-Silva, T., de Lima, L. A. G., Chaves-Silveira, J., Amado, T. F., Naipauer, J., Riul, P., and Martinez, P. A. 2021. Ecological and biogeographic processes drive the proteome evolution of snake venom. *Global Eco Biogeo*, 30(10): 1978–1989.

Slagboom, J., Kool, J., Harrison, R. A., and Casewell, N. R. 2017. Haemotoxic snake venoms: Their functional activity, impact on snakebite victims and pharmaceutical promise. *Br J Haematol*, 177(6): 947–959.

Smiley-Walters, S. A., Farrell, T. M., and Gibbs, H. L. 2017. Evaluating local adaptation of a complex phenotype: Reciprocal tests of pigmy rattlesnake venoms on treefrog prey. *Oecologia*, 184(4): 739–748.

Smith, C. F., Nikolakis, Z. L., Ivey, K., Perry, B. W., Schield, D. R., Balchan, N. R., Parker, J., Hansen, K. C., Saviola, A. J., Castoe, T. A., and Mackessy, S. P. 2023. Snakes on a plain: Biotic and abiotic factors determine venom compositional variation in a wide-ranging generalist rattlesnake. *BMC Biol*, 21(1): 136.

Straight, R. C., Glenn, J. L., Wolt, T. B., and Wolfe, M. C. 1991. Regional differences in content of small basic peptide toxins in the venoms of Crotalus adamanteus and Crotalus horridus. *Comp Biochem Physiol*, 100(1): 51–58.

Straight, R. C., glenn, J. L., Wolt, T. B., and Wolfe, M. C. 1992. North-south regional variation in phospholipase a activity in the venom of crotalus ruber. *Comp Biochem Physiol*, 103(3): 635–639.

Strickland, J. L., Smith, C. F., Mason, A. J., Schield, D. R., Borja, M., Castañeda-Gaytán, G., Spencer, C. L., Smith, L. L., Trápaga, A., Bouzid, N. M., Campillo-García, G., Flores-Villela, O. A., Antonio-Rangel, D., Mackessy, S. P., Castoe, T. A., Rokyta, D. R., and Parkinson, C. L. 2018. Evidence for divergent patterns of local selection driving venom variation in Mojave Rattlesnakes (Crotalus scutulatus). *Sci Rep*, 8(1): 17622.

Summers, K., Cronin, T. W., and Kennedy, T. 2003. Variation in spectral reflectance among populations of Dendrobates pumilio, the strawberry poison frog, in the Bocas del Toro Archipelago, Panama. *J Biogeo*, 30(1): 35–53.

Suryamohan, K., Krishnankutty, S. P., Guillory, J., Jevit, M., Schröder, M. S., Wu, M., Kuriakose, B., Mathew, O. K., Perumal, R. C., Koludarov, I., Goldstein, L. D., Senger, K., Dixon, M. D., Velayutham, D., Vargas, D., Chaudhuri, S., Muraleedharan, M., Goel, R., Chen, Y.-J. J., Ratan, A., Liu, P., Faherty, B., de la Rosa, G., Shibata, H., Baca, M., Sagolla, M., Ziai, J., Wright, G. A., Vucic, D., Mohan, S., Antony, A., Stinson, J., Kirkpatrick, D. S., Hannoush, R. N., Durinck, S., Modrusan, Z., Stawiski, E. W., Wiley, K., Raudsepp, T., Kini, R. M., Zachariah, A., and Seshagiri, S. 2020. The Indian cobra reference genome and transcriptome enables comprehensive identification of venom toxins. *Nat Genet*, 52(1): 106–117.

Templ, M., Hron, K., Filzmoser, P., Facevicova, K., Kynclova, P., Walach, J., Pintar, V., Chen, J., Miksova, D., Meindl, B., Menafoglio, A., Blasi, A. D., Pavone, F., Stefelova, N., Zeni, G., and Wiederkehr, R. 2023. robCompositions: Compositional Data Analysis.

Terhorst, J., Kamm, J. A., and Song, Y. S. 2017. Robust and scalable inference of population history from hundreds of unphased whole genomes. *Nat Genet*, 49(2): 303–309.

Tsai, I.-H., Wang, Y.-M., and Chen, Y.-H. 2003. Variations of Phospholipases A2 in the Geographic Venom Samples of Pitvipers. *J Toxicology*, 22(4): 651–662.

van den Wollenberg, A. L. 1977. Redundancy analysis an alternative for canonical correlation analysis. *Psychometrika*, 42(2): 207–219.

Vincent, S. E. and Mori, A. 2008. Determinants of feeding performance in free-ranging pit-vipers (Viperidae: Ovophis okinavensis): Key roles for head size and body temperature. *Bio J Linnean Soc*, 93(1): 53–62.

Vonk, F. J., Casewell, N. R., Henkel, C. V., Heimberg, A. M., Jansen, H. J., McCleary, R. J. R., Kerkkamp, H. M. E., Vos, R. A., Guerreiro, I., Calvete, J. J., Wüster, W., Woods, A. E., Logan, J. M., Harrison, R. A., Castoe, T. A., de Koning, A. P. J., Pollock, D. D., Yandell, M., Calderon, D., Renjifo, C., Currier, R. B., Salgado, D., Pla, D., Sanz, L., Hyder, A. S., Ribeiro, J. M. C., Arntzen, J. W., van den Thillart, G. E. E. J. M., Boetzer, M., Pirovano, W., Dirks, R. P., Spaink, H. P., Duboule, D., McGlinn, E., Kini, R. M., and Richardson, M. K. 2013. The king cobra genome reveals dynamic gene evolution and adaptation in the snake venom system. *Proc Natl Acad Sci*, 110(51): 20651–20656.

Webber, M. M., Jezkova, T., and Rodríguez-Robles, J. A. 2016. Feeding Ecology of Sidewinder Rattlesnakes, Crotalus cerastes (Viperidae). *Herpetologica*, 72(4): 324–330.

Werner, E. E. and Gilliam, J. F. 1984. The Ontogenetic Niche and Species Interactions in Size-Structured Populations. *Annual Rev Eco Syst*, 15(1): 393–425.

Westeen, E. P., Escalona, M., Holding, M. L., Beraut, E., Fairbairn, C., Marimuthu, M. P. A., Nguyen, O., Perri, R., Fisher, R. N., Toffelmier, E., Shaffer, H. B., and Wang, I. J. 2023. A genome assembly for the southern Pacific rattlesnake, Crotalus oreganus helleri, in the western rattlesnake species complex. *Journal of Heredity*, 114(6): 681–689.

Williams, B. L., Brodie, Jr., E. D., and Brodie, III, E. D. 2003. Coevolution of Deadly Toxins and Predator Resistance: Self-Assessment of Resistance by Garter Snakes Leads to Behavioral Rejection of Toxic Newt Prey. *Herpetologica*, 59(2): 155–163.

Williams, B. L., Hanifin, C. T., Brodie, E. D., and Brodie III, E. D. 2010. Tetrodotoxin affects survival probability of rough-skinned newts (Taricha granulosa) faced with TTX-resistant garter snake predators (Thamnophis sirtalis). *Chemoecology*, 20(4): 285–290.

Williams, V., White, J., Schwaner, T. D., and Sparrow, A. 1988. Variation in venom proteins from isolated populations of tiger snakes (Notechis ater niger, N. scutatus) in South Australia. *Toxicon*, 26(11): 1067–1075.

Wray, K. P., Margres, M. J., Seavy, M., and Rokyta, D. R. 2015. Early significant ontogenetic changes in snake venoms. *Toxicon*, 96: 74–81.

Wright, S. 1931. Evolution in Mendelian Populations. *Genetics*, 16(2): 97–159.

Wright, S. 1943. Isolation by Distance. *Genetics*, 28(2): 114.

Yang, Y., Servedio, M. R., and Richards-Zawacki, C. L. 2019. Imprinting sets the stage for speciation. *Nature*, 574(7776): 99–102.

Yin, W., Wang, Z.-J., Li, Q.-Y., Lian, J.-M., Zhou, Y., Lu, B.-Z., Jin, L.-J., Qiu, P.-X., Zhang, P., Zhu, W.-B., Wen, B., Huang, Y.-J., Lin, Z.-L., Qiu, B.-T., Su, X.-W., Yang, H.-M., Zhang, G.-J., Yan, G.-M., and Zhou, Q. 2016. Evolutionary trajectories of snake genes and genomes revealed by comparative analyses of five-pacer viper. *Nat Commun*, 7: 13107.

Zhang, J. 2018. Neutral Theory and Phenotypic Evolution. *Mol Biol Evol*, 35(6): 1327–1331.

Zhao, H.-Y., Sun, Y., Du, Y., Li, J.-Q., Lv, J.-G., Qu, Y.-F., Lin, L.-H., Lin, C.-X., Ji, X., and Gao, J.-F. 2021. Venom of the Annulated Sea Snake Hydrophis cyanocinctus: A Biochemically Simple but Genetically Complex Weapon. *Toxins*, 13(8): 548.